Prepublished Copy

NATURE ENVIRONMENT AND POLLUTION TECHNOLOGY

Article In Press

PEER-REVIEWED PREPUBLISHED MANUSCRIPT

This is a peer-reviewed prepublished version of the paper to be published in **Vol. 26, No. 1, March 2027.**

Assessment of water resources quality for multiple purposes in parts of the Volta basin in northern Togo, using chemometric-based indices

Nanoua Assani Amaté, Kossitse Venyo Akpataku, Gnon Baba, Waris Chouti, Kwamivi N. Ségbéaya

RECEIVED
15 April 2026

CITE THIS ARTICLE
Amaté, N.A., Akpataku, K.V., Baba, G., Chouti, W. and Ségbéaya, K.N., 2027. Assessment of water resources quality for multiple purposes in parts of the Volta basin in northern Togo, using chemometric-based indices. Nature Environment and Pollution Technology, 26(1), D1933.

https://doi.org/10.46488/NEPT.2027.v26i01.D1933

EARLY-ACCESS STATEMENT

This manuscript, after peer review, is being released online in its original, unedited form to provide early access to its findings. Prior to final publication, it will undergo additional editing and formatting. Readers may note that, as an unedited version, the manuscript may have linguistic and other minor errors. The DOI will be active after the final publication of the paper.

PUBLICATION STATUS

PEER REVIEW	ONLINE VERSION	FINAL ISSUE
Completed	Prepublished	March 2027

Type of the Paper (Original Research)

Assessment of water resources quality for multiple purposes in parts of the Volta basin in northern Togo, using chemometric-based indices

Nanoua Assani Amaté [1,2,3]†, Kossitse Venyo Akpataku[1], Gnon Baba[1,2], Waris Chouti[3], Kwamivi N. Ségbéaya[1]

[1]Laboratory of Organic Chemistry and Environmental Sciences, University of Kara, Kara B.P.404, Togo

[2]Laboratory of Waste Management, Treatment and Valorization (GTVD), University of Lomé, Lomé 01 B.P. 1515 Lomé 01, Togo

[3]Laboratory of Chemistry, Physics, Materials and Molecular Modeling, University of Abomey-Calavi, Cotonou 01 BP 526, Benin

†**Corresponding Author**: Nanoua Assani Amaté; assaninanoua@gmail.com

Abstract

Water quality assessment is essential for its sustainable use. Therefore, this study evaluates the quality of water resources in the Togolese portion of the Volta Basin by combining physicochemical analyses, chemometric indices, and multivariate statistical methods. A total of 115 samples from surface water, groundwater, and tap water were collected at the end of the rainy season (October 2024) and during the dry season (February 2025). Selected hydrochemical parameters have been determined using standard methods. The Water Quality Index (WQI) and conventional hydrogeochemical approaches have been applied to examine the health of groundwater resources and the controlling drivers. The results revealed that surface waters experience low mineralization during the wet season, whereas groundwater shows increased mineralization associated with infiltration and mineral dissolution. The Water Quality Index shows that only tap water maintains consistently potable quality, unlike surface water and groundwater, whose quality was unsuitable at 70% and 21%, respectively, during the rainy season, against 47% and 10% in the dry season. Principal Component Analysis reveals three major gradients controlling water quality: natural silicate and accessory minerals weathering, nitrogen-based anthropogenic inputs, and metal contamination. Bivariate analysis indicates that mineralization is mainly controlled by silicate weathering, carbonate dissolution, and ion exchange processes, while the low concentrations of Cl^- and SO_4^{2-} rule out any significant evaporitic influence. Irrigation indices indicate that most waters are dominated by sodium and magnesium. Industrial stability indices highlight varying corrosion and scaling risks by site and season. These findings provide essential insights for the sustainable and integrated management of water resources in the Volta Basin.

Key words: seasonal water quality; water suitability; geochemical processes; hydrochemistry; Volta Basin, Togo

1. Introduction

Freshwater resources, which account for less than 3% of the global water reserves, are essential for domestic, agricultural, and industrial development (Akhtar et al., 2021). However, their availability and quality are increasingly threatened by climate change and human activities such as intensive agriculture, rapid urbanisation, and the development of hydraulic and societal infrastructures (Burri et al., 2019; Xiao et al., 2025). Population growth further exacerbates this pressure, leading to a marked deterioration in water quality, particularly in developing countries, where water bodies are exposed to multiple sources of contamination, most of the time related to anthropogenic activities (Akpataku et al., 2025a; Ouedraogo et al., 2020; Segbeaya et al., 2019).

Overexploitation, agricultural practices, industrial discharges, and improper waste management are the main drivers of groundwater quality deterioration. Due to connections between the environmental matrix through the hydrologic cycle, it becomes difficult to protect water resources by stopping the migration of contaminants from their sources to rivers and groundwater. Ensuring the quality of water resources is a central challenge for sustainable development, particularly in Africa, where communities rely heavily on groundwater and surface water to meet their daily needs and to achieve the Sustainable Development Goals (SDGs) related to poverty reduction, public health, and the protection of aquatic ecosystems(George-Williams et al., 2024; McClain, 2013). In this context, the long-term sustainability of water quality depends on the implementation of transdisciplinary and transboundary actions, supported by local and community participation and collaborative governance, to ensure equitable access to water resources and the long-term protection of water quality (Burri et al., 2019; Ogbekene, 2025).

In West Africa, the Volta Basin represents a major hydrological system that supports millions of inhabitants (GWP, 2019). It supports a complex interplay between growing water demands, climatic variability, and the challenges of coordinating governance across multiple national borders (Owusu et al., 2025). Assessing water quality in the Volta Basin is essential for resource development and sustainable management, particularly in the Togolese part, where hydrogeochemical investigations are less documented (Akpataku et al., 2025b) than in other parts, such as Ghana (Lartsey et al., 2024; Loh et al., 2012; Sunkari et al., 2024).

Yet, water resources are increasingly exposed to anthropogenic pressures, including population growth, expanding agricultural activities, and inadequate waste management in the basin. In northern Togo, there is a rise in domestic and agricultural water demand, coupled with insufficient management of domestic, urban, and industrial waste, as well as agricultural effluents (Barry et al., 2025). This can promote excessive transfer of mineral and organic substances into surface and groundwater, compromising the physical, chemical, and microbiological quality of water resources and thereby affecting drinking water supply, agricultural and livestock production, and industrial use.

Assessing water quality in such a context requires comprehensive and robust analytical approaches that capture the complexity of hydrochemical processes and the multiple constraints associated with water use (Nosrati, 2017; Sodomon et al., 2025). Chemometric-based indices, such as the Water Quality Index (WQI) for drinking purposes (Renu Nayar, 2020; Çadraku and Beqiraj, 2023; Kumar and Maurya, 2025) and irrigation (Kumar et al., 2024; Rehman et al., 2024; Tegegne et al., 2023) and industrial suitability indices (Dehghani et al., 2019; Kumar et al., 2024), provide powerful tools for transforming complex datasets into meaningful classifications and management insights. When combined with multivariate statistical techniques, these methods help assess water quality, pollution sources, hydrochemical characteristics, and control, as well as the suitability and sustainability of water resources for various uses (Patel et al., 2023). Their effectiveness for drinking has been demonstrated worldwide, including in India in the groundwater of Tumkur Taluk (Ramakrishnaiah et al., 2009), in Turkey on the Aksu River (Şener et al., 2017), and in Thailand (Bordalo et al., 2001). In Africa, the use of the water quality index has also yielded convincing results, as in Algeria (Mammeri et al., 2023), Morocco (Bekri et al., 2020), and southeastern Togo (Napo et al., 2021; Tampo et al., 2022). These indicators for irrigation and industrial use have been successfully applied in various regions, including arid and semi-arid environments, to classify water and guide sustainable irrigation practices (Kumar et al., 2024; Nsabimana and Li, 2023).

Despite the strategic importance of the Volta Basin (UNEP-GEF, 2010), comprehensive assessments of water quality integrating both seasonal and multipurpose dimensions remain scarce in northern Togo. This lack of information limits the development of effective, long-term management strategies that ensure sustainable and equitable water resource use. Addressing this gap requires evaluating water quality through an integrated approach combining physicochemical analyses, chemometric indices, and multivariate statistics.

Therefore, this study aims to assess, on a seasonal basis, the quality of water resources in parts of the Volta Basin in northern Togo using an integrated framework that incorporates physicochemical characterization, chemometric-based water-quality indices, and multivariate statistical methods. The specific objectives are the following: (i) to assess the seasonal variation of the physicochemical characteristics of water resources in the study area, (ii) to determine the water resources hydrochemical facies, (iii) to identify the drivers and geochemical processes controlling water resources mineralization, and (iv) to appraise the suitability of water resources for drinking, irrigation, and industrial use. The findings are essential for providing insights into seasonal variations in water quality, identifying potential contamination sources, and supporting objective-based recommendations for sustainable and equitable water resources management in the study area.

2. Materials and methods

2.1 Study area

The study was conducted in the northern part of the Volta Basin in Togo (Fig 1). The study area is characterized by a Sudanian-Sudano-Guinean climate type, with a unimodal rainfall regime (Badjana et al., 2017), a rainy season from April to October, and a long dry season from November to March. Within this climatic context, mean annual rainfall ranges from 1,000 to 1,200 mm, while average temperatures range from 25.4 °C to 31.6 °C.

Several socioeconomic activities are identified in the Volta Basin region; among these, agriculture is the dominant activity, employing a large part of the population. Market gardening, characterized by the intensive use of agricultural inputs, and livestock farming, through the production of animal waste, contribute to the economy of the Volta Basin in Togo. Land degradation is widespread at the national level, representing almost 5% over the last few decades. Population growth is putting increased pressure on land, encouraging its conversion into agricultural and residential areas. Farmers are gradually exploiting available land for food production, while urbanization is expanding to meet housing needs, highlighting the interdependence between agriculture and urbanization, as population growth drives the expansion of cultivated and settlement areas.

From a hydrological perspective, the drainage network is dominated by the Oti River, the only perennial river in the region, together with its main tributaries, including the Kara, Koumongou, Kéran, Mô, and Koulougouna rivers (Koukou-Tchamba, 2022; UNEP-GEF, 2010). The basin morphology is organized along a south-north gradient, with the basin progressively widening (UNEP-GEF Volta Project, 2013). This organization results from a structural framework dominated by the succession of the Birimian crystalline basement, the Oti (Buem) sedimentary basin, and the Atakora orogenic belt, forming an assemblage recognized as one of the oldest and most stable geological units in West Africa (Affaton, 1987; Block et al., 2016; Gebrechorkos et al., 2022; Tairou et al., 2022). The southeastern part of the study area is characterized by an association of metasedimentary, metamorphic, and crystalline rocks belonging to both the Volta sedimentary basin and the Pan-African Dahomeyide Belt. In the extreme western part of the area, metasedimentary rocks crop out. They are mainly composed of fine- to medium-grained feldspathic and clayey sandstones, locally micaceous (greywackes), as well as pelites. Furthermore, these formations overlie the external units of the Dahomeyide Belt, formed during the Pan-African orogeny. From west to east, the Buem structural unit, dominated by quartzitic sandstones and hematitic formations associated with tillites, is followed by the Atakora structural unit, which is mainly composed of schists and quartzites.

The population depends mainly on discontinuous fractured aquifer systems, whose hydraulic conductivity is controlled by secondary fracture permeability developed by weathering processes. The weathering profile is known to be mainly composed of a saprolite layer that provides groundwater storage and a fissured bedrock that affords adequate transmissivity to sustain well discharges (Lachassagne et al., 2021). In the study area, the weathering thickness is usually variable. Still, it is lower than 40 m bgl, with values between 5 and 10 m being the most frequent, depending on the rock's silica content and the degree of erosion (Ani et al., 2025). Later authors found no relationship between the distribution of discharge measured at drilling and the weathering thickness. Borehole depths are between 20 m and 120 m bgl, with linear discharge ranging from 6.10^{-3} to $9.10^{-1} m^3/h/m$ and the depth range from 24 to 52 m, corresponding to the most productive zone of the aquifer system (Ani et al., 2025a). The hydrodynamic characteristics are variable, reflecting the hydraulic heterogeneity of the aquifer systems. The parameters such as drilling discharge, specific discharge, and transmissivity vary from 0.1 to 40 m^3/h, 0.02 to 5.2 $m^3/h/m$, and $5.9\ 10^{-7}$ to $6.2\ 10^{-3}\ m^2/s$, respectively (Ani et al., 2025; Goumpoukini et al., 2019). The average depth to water level is around 10.0 ± 6.1 m bgl, with the main piezometric domes at high altitudes. As in most tropical basement settings, water flow is controlled by geomorphology from high to low altitudes, converging into the rivers' main courses (Ani et al., 2025; Akpataku et al., 2019).

2.2 Sampling procedures and *in-situ* measurements

Two seasonal sampling campaigns were conducted as part of this study. At the end of the rainy season (October 2024), a total of 56 water samples (Fig 1) were collected, including 42 groundwater samples, 10 surface water samples, and 4 tap water samples. During the dry season (February 2025), A total of 59 samples were collected: 39 groundwater, 15 surface water, and 5 tap water. To ensure comparability between seasons, the same sampling sites were systematically revisited during both campaigns. In addition, sampling points were added in certain areas to improve the study's spatial coverage.

All samples were collected in pre-cleaned high-density polyethylene bottles with a capacity of 1 Liter and stored in coolers at 4 °C before transport to the laboratory for chemical analysis. During sampling, an aliquot of 100 mL from each sample was filtered through 0.45 µm nitrocellulose membranes and acidified to pH < 2 with ultrapure nitric acid to allow cation analyses (Ndoye et al., 2023).

The latitude and longitude of each sampling location were approximated using MAPS.ME for geolocation. Sartorius PT-10 pH meter and an ELMETRON CC-411 conductivity meter, both calibrated beforehand, were used for *in situ* measurements of pH (± 0.1), electrical conductivity (± 0.25%), and temperature (± 0.1°C). These measurements were taken directly in the field to minimize any alteration of the samples' characteristics.

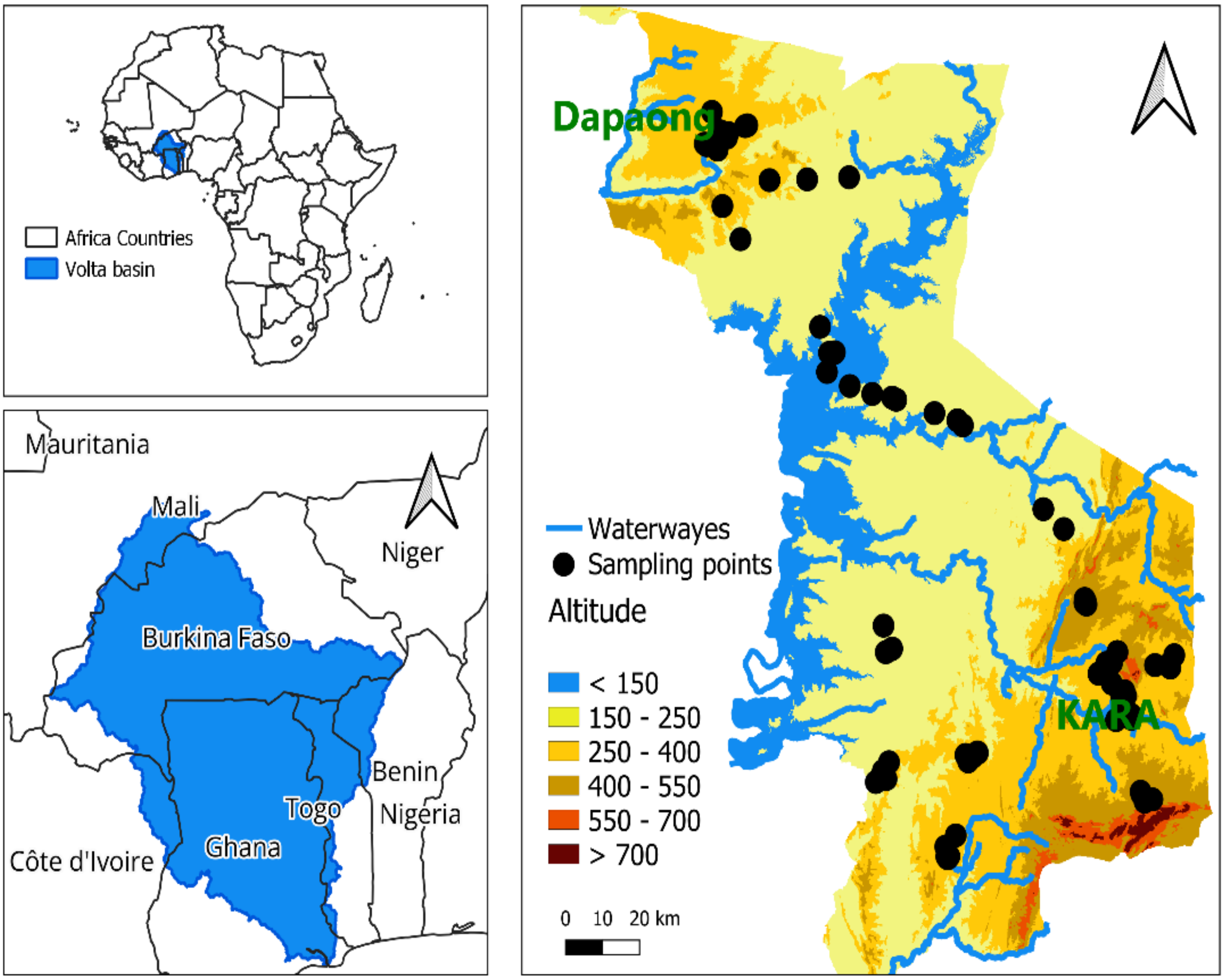

Fig 1 : Map showing study area location and sampling points

2.3 Analyses of physicochemical parameters

In the laboratory, the physicochemical parameters were measured according to the protocol described by

Rodier et al. (2009). The concentrations of HCO_3^- (± 0.6 mg/L), Cl^- (± 0.35 mg/L), Ca^{2+} (± 0.4 mg/L), and Mg^{2+} (± 0.24 mg/L) ions were determined by volumetry. NO_3^-, NO_2^-, PO_4^{3-}, SO_4^{2-} , and NH_4^+ ions were measured by UV-visible spectrophotometry (Genesys 10S UV-Vis), with an uncertainty of ± 1 to 2% (Sodomon et al., 2025). The K^+, Na^+, and total iron contents were measured by inductively coupled plasma optical emission spectrometry (ICP-OES), with a detection limit of less than 0.002 mg/L (Manu et al., 2023). The oxidability (permanganate index PI) was determined by permanganate oxidation, with an uncertainty of ± 0.1 mg O_2/L.

Before using the chemical data from all samples, they were subjected to ion balance error (IBE) calculations to assess the accuracy of the chemical analysis for each water sample. The IBE values were within the acceptable ±10% limit for all samples, validating the use of their chemical data for interpretation. (El Baba et al., 2020; Giri et al., 2025). The Ion Balance Error (IBE) is calculated using Equation (1).

$$IBE = \frac{\sum Cation - \sum Anions}{\sum Cation + \sum Anions} * 100 \quad (1)$$

2.4 Statistical analysis

Before statistical analysis, all physicochemical data were standardized to ensure comparability among variables and to avoid distortions related to differences in measurement scales. Descriptive statistics and the Mann-Whitney U test were applied to seasonal and water-source groups at a 95% confidence level to identify variations across the different seasons. In addition, principal component analysis (PCA), aimed at reducing data dimensionality and identifying the major factors or drivers explaining the overall variance in the dataset, was performed, along with correlation analyses, using OriginPro 2021 (Huang et al., 2010; Ma et al., 2020). In parallel, correlation analyses were conducted to characterize the relationships among water quality parameters. These multivariate analyses made it possible to investigate the simultaneous variations of physico-chemical parameters and to highlight dominant statistical structures, trends, and differences among samples, thereby contributing to a more comprehensive interpretation of water quality and hydrogeochemical evolution as detailed in previous studies (Sodomon et al., 2025; Sunkari et al., 2024; Hamma et al., 2024; Patel et al., 2023; Akpataku et al., 2020).

Furthermore, the assessment of hydrogeochemical processes controlling the chemical composition of groundwater and surface water was based on the combined use of classical hydrochemical diagrams and geochemical analysis tools. The Piper diagram was used to identify and classify hydrochemical facies based on the concentrations of major cations and anions (Piper, 1944). This approach allows discrimination of dominant water types and highlights mineralization processes associated with water-rock interactions and other interactions. The integration of these approaches provides a comprehensive understanding of the mechanisms controlling the chemical composition and quality of the studied waters.

2.5 Water quality index

To assess current water quality and potential uses of water resources in the Volta Basin, a water quality

index (WQI) was applied to a dataset collected specifically for this study (Bordalo et al., 2001). This index reflects the combined influence of various water quality parameters on potability and summarises overall quality status in a single indicator by comparing each parameter with international reference standards.

The WQI was calculated using the method developed by Brown et al. (1972), which was adopted by Horton (1985) and Tyagi et al. (2020). This widely used method is based on Equations 2-5. Each quality parameter is weighted according to a relative weight (Wi) (Equation 2). This weighting is based on the maximum value recommended by the World Health Organization (WHO) for each parameter, denoted as Si (in mg/L), except for pH and electrical conductivity. The constant K (Equation 3) represents the proportionality constant, and n the total number of parameters considered. The following formula then expresses the overall calculation of the index:

$$Wi = \frac{K}{S_i} \tag{2}$$

$$K = \frac{1}{\sum_{i=1}^{n}\left(\frac{1}{Si}\right)} \tag{3}$$

W_i is the relative weight of each parameter, proportional to its importance for overall water quality.

S_i represents the maximum value recommended by the WHO for the parameter. The constant K is the proportionality constant, and n is the total number of parameters considered. The quality sub-index is determined following Equation 4.

$$Qi = \left|\frac{C_i - C_o}{S_i - C_o}\right| * 100 \tag{4}$$

Where Q_i is the quality sub-index for each parameter, calculated from the measured concentration.

C_i is the concentration of each parameter, and Co represents the minimum acceptable concentration for each parameter (Table 1).

The WQI is then obtained using the following Equation 5.

$$WQI = \frac{\sum_{i=1}^{n} Q_i W_i}{\sum_{i=1}^{n} W_i} \tag{5}$$

The relative weight calculation and minimum acceptable concentration for each parameter are presented in Table 1.

Table 1 : Calculation parameters and weighting factors used for Water Quality Index (WQI)

	WHO guidelines(S_i)	1/Si	∑1/Si	K= 1/(∑1/Si)	Wi=K/Si	Ideal Value Co
pH	8.5	0.12	4.61	0.22	0.03	7.00
TDS (mg/L)	500	0.00	4.61	0.22	0.00	0
HCO_3^- (mg/L)	200	0.01	4.61	0.22	0.00	0
Ca^{2+} (mg/l)	75	0.01	4.61	0.22	0.00	0
Mg^{2+} (mg/L)	50	0.02	4.61	0.22	0.00	0
K^+ (mg/l)	12	0.08	4.61	0.22	0.02	0
Na^+ (mg/l)	200	0.01	4.61	0.22	0.00	0
Fer (mg/L)	0.3	3.33	4.61	0.22	0.72	0
NH_4^+ (mg/L)	1.5	0.67	4.61	0.22	0.14	0
NO_3^- (mg/L)	50	0.02	4.61	0.22	0.00	0
NO_2^- (mg/L)	3	0.33	4.61	0.22	0.07	0
Cl^-(mg/L)	250	0.00	4.61	0.22	0.00	0
SO_4^{2-} (mg/L)	250	0.00	4.61	0.22	0.00	0
	∑1/Si	4.61			1.00	

The WQI rating is summarized in Table 2. Showing a low WQI for good water quality, while a high WQI reflects poor or deteriorated water quality.

Table 2: Water Quality Index (WQI) classification ranges

WQI	Water resource quality	Use
0-25	Excellent quality	Drinking water
>25-50	Good quality	Drinking water
>50-75	Poor quality	Use in irrigation and industry
>75-100	Very poor quality	Use in irrigation
>100	Non-potable water	Appropriate treatment is required before use

2.6 Water quality for irrigation purposes

Table 3 summarizes the calculation methods (Equations 6-12), where all ion concentrations are expressed

in meq/L.

The Irrigation Water Quality Index is designed to evaluate the suitability of water resources for

agricultural irrigation. In this study, seven parameters namely Sodium Adsorption Ratio (SAR), Sodium Percent (Na%), Residual Sodium Carbonate (RSC), Kelly's Ratio (KR), Magnesium Hazard (MH), Permeability Index (PI) and Potential Salinity (PS) (Table 3), were used to classify the sampled water in terms of its appropriateness for irrigation purposes (Rehman et al., 2024).

Table 3: Classification ranges for irrigation water quality indices

	Equation		Rang	Category	
SAR	$SAR = \frac{[Na^+]}{\sqrt{\frac{([Ca^{2+}) + [Mg^{2+}])}{2}}}$	(6)	<10 10-18 18-26 >26	Excellent Good Acceptable Unacceptable	(Tegegne et al., 2023)
%Na	$\% Na = 100 * \frac{[Na^+] + [K^+]}{[Ca^{2+}] + [Mg^{2+}] + [Na +] + [K +]}$	(7)	<20% 20-40% 40-60% 60-80% 80-100%	Excellent quality Good quality Medium quality Poor quality Unsuitable quality	(Kawo and Karuppannan, 2018)
RSC	$RSC = ([HCO_3^-] + [CO_3^{2-}]) - ([Ca^{2+}] + [Mg^{2+}])$	(8)	<1.25 1.25-2.5 >2.5	Good quality Poor quality Unsuitable quality	(Peiyue et al., 2011)
KR	$KR = \frac{[Na^+]}{[Ca^{2+}] + [Mg^{2+}]}$	(9)	<1 >1	Suitable Unsuitable	(Kumar et al., 2024)
MH	$MH = 100\frac{[Mg^{2+}]}{[Ca^{2+}] + [Mg^{2+}]}$	(10)	<50 >50	Suitable Unsuitable	(Kumar et al., 2024)
PI	$PI = 100 * \frac{[Na^+] + \sqrt{[HCO_3^-]}}{[Ca^{2+}] + [Mg^{2+}] + [Na^+]}$	(11)	<25 25-75 >75	Unsuitable Good Suitable	(Eid et al., 2023)
PS	$PS = [Cl^-] + \frac{[SO_4^{2-}]}{2}$	(12)	<3 3-5 >5	Suitable Good Unsuitable	(Eid et al., 2023)

2.7 Water quality for industrial purposes

The suitability of water for industrial use can be evaluated by assessing its corrosivity and scaling potential using several industrial water-stability indices (Table 4). These indices, such as the Langelier Saturation Index (LSI), Ryznar Stability Index (RSI), Puckorius Scaling Index (PSI), and the Larson-Skold Index (LI), provide quantitative estimates (Equations 13-22) of the tendency of water to cause corrosion or scale formation in industrial systems.

Table 4: Classification ranges for industrial suitability indices

			Rang	Category	
LSI	$LSI = pH - pHs$	(13)	<0	Corrosive	(Mahaqi et al., 2018)
	$pHs = (9.3 + A + B) - (C + D)$	(14)			
	$A = \log_{10}(TDS - 1)/10$	(15)	0±0.5	Stable	
	$B = -13.12 * \log_{10}[T(°C) + 273] + 34.55$	(16)			
	$C = \log_{10}([Ca^{2+}])$	(17)			
	$D = \log_{10}([HCO_3^-])$	(18)	>0.5	Scaling	
PSI	$PSI = 2pHs - pHeq$	(19)	<5	Scaling	(Kumar et al., 2022)
	$pHeq = 1.465 * \log_{10}(Alcanity\ CaCO_3) + 4.54$	(20)	5-6	Slight scaling	
			>8	Corrosive	
RSI	$RSI = 2pHs - pH$	(21)	<6	Scaling forming	(El Baroudi et al., 2024)
			6-7	Stable	
			>7	Corrosive	
LI	$LI = \frac{[Cl^-] + [SO_4^{2-}]}{[CO_3^{2-}] + [HCO_3^-]}$	(22)	<0.8	Safe	(Ahmed et al., 2021)
			0.8-1.2	Slight	
			>1.2	High corrosion risk	

3 Results and discussion

3.1 Seasonal variation of hydrochemical characteristics

Tap water (Table 5) temperature ranged from 30.35 ± 1.60 °C during the rainy season to 31.66 ± 4.32

°C during the dry season. The pH values averaged 6.81 ± 0.80 in the rainy season and 7.10 ± 0.13 in the dry season. These pH values indicate generally neutral water, with limited seasonal variability. Electrical conductivity (EC) varied from 287 ± 149 µS/cm in the rainy season to 321 ± 200 µS/cm in the dry season, reflecting a moderate degree of mineralization influenced by both the nature of the water sources and treatment processes. Total hardness (TH) exhibited more pronounced seasonal variations, decreasing from 102.04 ± 40.42 mg/L as $CaCO_3$ during the rainy season to 45.84 ± 26.19 mg/L as $CaCO_3$ during the dry season. Sodium (Na^+) and potassium (K^+) concentrations remained well below the World Health Organization (WHO) guideline values of 200 mg/L and 12 mg/L, respectively.

Bicarbonate ions (HCO_3^-) increased during the dry season (90.49 ± 99.33 mg/L) compared with the rainy season (56.73 ± 62.84 mg/L). Chloride concentrations (Cl^-) decreased from 55.03 ± 14.64 mg/L in the rainy season to 15.92 ± 11.03 mg/L in the dry season. Sulphate concentrations (SO_4^{2-}) remained low to moderate, with values of 19.72 ± 9.68 mg/L during the rainy season and 19.62 ± 19.88 mg/L during the dry season.

While ammonium (NH_4^+) and nitrite (NO_2^-) concentrations remained below the detection limit of the analytical instrument, nitrate (NO_3^-) concentrations varied from 5.28 ± 5.45 mg/L in the rainy season to 0.48 ± 0.05 mg/L in the dry season. Finally, the permanganate index (PI), used as an indicator of organic matter pollution, showed low values in both the rainy (1.30 ± 0.64 mgO_2/L) and dry (1.01 ± 0.68 mgO_2/L) seasons.

Table 5 : Descriptive statistical summary of physicochemical parameters for Tap water

Tap water samples									WHO guidelines
Parameters	End of rainy season (n=4)				Dry season (n=5)				
	Min	Mean	Max	SD	Min	Mean	Max	SD	
T° C	28.20	30.35	31.80	1.60	24.80	31.66	36.70	4.32	-
pH	5.64	6.81	7.42	0.80	6.93	7.10	7.27	0.13	6.5 à 8.5
EC (µS/cm)	188	287	507	149	113	321	624	200	-
TDS(mg/L)	122	186	330	97	74	209	406	130	-
TH (mg/L CaCO3)	67.60	102.04	160.57	40.42	15.00	45.84	80.40	26.19	-
Ca^{2+} (mg/L)	2.00	4.30	6.80	2.45	2.40	9.76	18.40	5.98	75
Mg^{2+} (mg/L)	15.20	22.17	35.35	9.02	1.94	5.23	8.40	3.13	50
K^+ (mg/L)	1.40	2.59	4.67	1.44	1.61	3.15	5.39	1.93	-
Na^+ (mg/L)	2.27	20.46	36.41	17.94	5.71	25.59	87.80	35.10	12
FeT (mg/L)	0.02	0.14	0.31	0.14	0.01	0.06	0.22	0.11	200
NH_4^+ (mg/L)	0.25	0.25	0.25	-	0.25	0.25	0.25	-	0.3
Cl^- (mg/L)	35.50	55.03	71.00	14.64	3.50	15.92	28.40	11.03	1.5
HCO_3^- (mg/L)	18.30	56.73	150.67	62.84	21.35	90.49	258.76	99.33	50
SO_4^{2-} (mg/L)	13.25	19.72	34.00	9.68	1.94	19.62	44.18	19.88	3

NO_3^- (mg/L)	0.95	5.28	13.23	5.45	0.38	0.48	0.50	0.05	250
NO_2^- (mg/L)	0.03	0.03	0.03	-	0.03	0.03	0.03	-	250
PI (mg O2 /L)	0.35	1.30	1.75	0.64	0.25	1.01	1.80	0.68	5

The analytical results for surface water (Table 6) are presented as statistical summaries. The results show

significant seasonal variability in the physical and chemical characteristics of surface water. Temperature increases significantly ($p < 0.05$) at the end of the rainy season compared to the dry season, probably due to the monsoon and winter characteristics of the weather during both sampling periods. However, the temperature of tap water did not vary significantly. During the rainy season, surface water bodies are likely to be exposed to higher ambient temperatures and higher solar radiation. The pH of surface water samples ranged from 7.0 to 8.0, with mean values around 7.2 and 7.5 at the end of the rainy and dry seasons, respectively, indicating that surface water remains generally neutral and shows no significant seasonal variation. The values are compliant with WHO drinking water standards (OMS, 2017). Electrical conductivity (EC) and TDS showed lower values during the rainy season (113 ± 47 µS/cm and 73 ± 30 mg/L) than during the dry season (152 ± 63 µS/cm and 99 ± 41 mg/L), reflecting a marked dilution effect from freshwater inputs from precipitation and runoff. Major ions such as calcium, magnesium, bicarbonates, and total hardness follow the same pattern and are significantly lower during the rainy season.

Table 6 : Descriptive statistical summary of physico-chemical parameters for surface water

Variables	Surface water samples											
	End of rainy season (n =10)					Dry season (n =15)						WHO guidelines
	Min	Mean	Max	SD	%CV	Min	Mean	Max	SD	%CV	P-value	
T°C	28.8	30.6	34.3	2.0	6.5	23.2	26.9	30.7	2.1	7.7	<0.05	-
pH	7.0	7.5	8.0	0.4	4.9	7.1	7.3	7.7	0.3	3.5	0.5	6.5 à 8.5
EC(µs/cm)	55	113	185	47	41	69	152	292	63	42	0.1	-
TDS(mg/L)	36	73	120	30.2	41	45.0	99	190	41	42	0.1	-
HCO_3 (mg/L)	2.0	11.8	18.3	5.6	47.9	4.7	28.3	80.2	20.0	70.7	<0.05	-
Ca^{2+} (mg/L)	<DL	2.5	4.4	1.4	54.9	1.1	5.1	13.6	3.9	75.3	0.1	75
Mg^{2+} (mg/L)	4.9	9.5	13.5	3.1	33.0	0.7	2.4	7.8	1.8	76.8	<0.05	50
TH(mg/L$CaCO_3$)	23.0	45.2	63.4	15.6	34.6	8.9	22.6	53.5	15.1	66.6	<0.05	-
K^+ (mg/L)	1.0	2.1	6.5	1.6	78.3	1.8	5.0	10.1	2.8	56.9	<0.05	12
Na^+ (mg/L)	1.6	3.6	6.2	1.5	42.8	3.1	10.5	34.0	8.4	79.9	0.1	200
FeT (mg/L)	<DL	1.6	4.1	1.3	82.0	0.1	0.8	1.8	0.7	90.0	0.3	0.3
NH_4^+(mg/L)	<DL	0.3	0.6	0.2	90.7	<DL	0.1	0.6	0.2	186.1	<0.05	1.5
NO_3^-(mg/L)	2.0	5.2	8.2	2.2	42.6	0.5	3.4	9.6	2.8	83.6	0.1	50
NO_2^-(mg/L)	<DL	0.2	0.5	0.2	97.2	<DL	0.1	0.2	0.1	110.9	<0.05	3

Cl^- (mg/L)	13.7	31.8	52.1	10.7	33.7		6.4	19.9	46.2	11.2	56.3	<0.05	250
SO_4^{2}(mg/L)	0.3	1.5	2.9	1.1	78.9		0.5	0.9	2.3	0.6	66.8	0.7	250
PI(mg O_2/L)	2.8	3.7	6.3	1.1	29.7		<DL	3.0	5.1	1.3	43.9	0.6	5

In contrast, some parameters increase during the rainy season. This is particularly evident for nutrients

such as nitrates (5.2 ± 2.2 mg/L), likely due to agricultural runoff, the transport of nitrogen fertilizers, and leaching from soils enriched in organic matter (Ayeni et al., 2023; Smith et al., 2020). Total iron (1.6 ± 1.3 mg/L) may also increase during this period, attributed to the remobilization of ferruginous soils or the suspension of iron-rich particles by rainfall (Ayeni et al., 2023; Silva et al., 2018). Chlorides (31.8 ± 10.7 mg/L) and sulfates (1.5 ± 1.1 mg/L) also show a slight increase during the rainy season, suggesting mineral inputs through runoff or disturbance of riverbed sediments. The permanganate oxidability index is higher in surface water than in groundwater during both seasons (Table 7), consistent with the likely higher organic matter and suspended particle content, as well as the greater abundance of reductant species, such as iron species.

Similar to surface water, groundwater (Table 7) shows little seasonal variation in EC and TDS. EC

averaged 527 ± 310 µS/cm at the end of the rainy season compared with 514 ± 304µS/cm during the dry season. However, several major ions show statistically significant seasonal variations ($p < 0.05$), notably magnesium, potassium, and sodium. Their concentrations increase significantly at the end of the rainy season: Mg^{2+} (41.2 ± 29.7 mg/L), K^+ (3.3 ± 3.0 mg/L), and Na^+ (101.3 ± 116.3 mg/L), whereas calcium (12.7 ± 8.5 mg/L) is more abundant during the dry season. This contrast may reflect the effect of aquifer recharge, whereby increased infiltration enhances the dissolution of minerals in the soil and bedrock, enriching groundwater with dissolved ions (Singh et al., 2024).

Bicarbonates also show higher values during the rainy season (131.4 ± 117.3 mg/L). Nutrients follow the same trend.

Nitrates increase significantly between seasons ($p < 0.05$), rising from an average of 12.5 mg/L in the dry season to 40.3 mg/L at the end of the rainy season. This substantial rise highlights the aquifer's high vulnerability to surface infiltration, particularly from agricultural fertilizers and domestic wastewater (Ben Moussa et al., 2019). Few groundwater sampling points exceed the WHO potability limit (50 mg/L), with concentrations up to 213.2 mg/L at the end of the rainy season, compared with 117.7 mg/L during the dry season, suggesting a potential health risk, particularly for children (OMS, 2017; UE, 2020; Akpataku et al., 2025a).

These results are consistent with those reported by Dougna et al. (2024) for the city of Kara in the study area, indicating that nitrate concentrations are higher in the rainy season than in the dry season. At the country level, other regional studies in basement aquifers have also reported seasonal variation in the anthropogenic impact on groundwater quality (Akpataku et al., 2025a; Sodomon et al., 2025). However, compared with the work of Zoulgami et al. (2015), which reported concentrations below 11 mg/L, the hypothetical threshold of anthropogenic influence (Akpataku et al., 2025a), the overall results suggest a deterioration in water quality in part of the study area. Such evolutions with emerging groundwater nitrate contamination, driven by changing phases in fast-growing communities, are observed in parts of the world where anthropogenic activities exert significant pressure on water resources (Anornu et al., 2017; Saka et al., 2023; Aju et al., 2024). Therefore, effective and adapted management options that integrate global approaches and perspectives are required in the study area to constrain groundwater contamination and use water resources sustainably.

Total iron also increases during the rainy season, with concentrations occasionally reaching high levels (13.3 mg/L), although this difference is not always statistically significant. This increase may result from the dissolution of ferruginous minerals under more reducing wet-season conditions or from particle-laden water infiltration, possibly linked to mining activities (Akpaki et al., 2019; Ayeni et al., 2023; Toi Bissang et al., 2024). Both chloride and sulfate ions increase slightly at the end of the rainy season. However, only chloride shows a statistically significant variation ($p < 0.05$), reaching up to 48.6 mg/L. The seasonal increase in chloride and the similar, though non-significant, trend in sulfates reflect enhanced inputs of dissolved elements from natural or anthropogenic sources (Koukou-Tchamba, 2022; Sodomon et al., 2025). Overall, groundwater exhibits a seasonal dynamic that is generally the opposite of that of surface water: it becomes more mineralized during the rainy season due to increased infiltration and dissolution. It shows a significant rise in nitrate and chloride concentrations, indicating pronounced vulnerability to contamination and human activities. The quality of groundwater can improve or deteriorate with the seasons, underscoring the importance of seasonal monitoring for sustainable management (Singh et al., 2024).

Table 7 : Descriptive statistical summary of physico-chemical parameters for groundwater

Variables	Groundwater samples											
	End rainy season (n = 42)					Dry season (n = 39)						WHO guidelines
	Min	Mean	Max	SD	%CV	Min	Mean	Max	SD	%CV	P-value	
T°C	25.0	30.5	34.2	2.0	6.6	25.0	29.8	35.8	2.2	7.3	0.2	-
pH	5.1	6.9	7.7	0.6	8.4	5.0	6.9	7.9	0.6	9.2	0.5	6.5 à 8.5
EC(µs/cm)	90	527	1 265	310	59	66	514	1 066	304	59	0.9	-
TDS(mg/L)	59	342	822	202	59	43	334	693	197	59	0.9	-
HCO_3 (mg/L)	0.6	131.4	411.8	117.3	89.3	0.6	167.1	392.8	122.8	73.5	0.2	-
Ca^{2+} (mg/L)	0.5	5.8	20.4	4.5	76.9	0.8	12.7	40.0	8.5	66.4	<0.05	75
Mg^{2+} (mg/L)	<DL	41.2	103.8	29.7	72.2	0.7	10.2	31.8	8.8	86.6	<0.05	50
TH (mg/L$CaCO_3$)	10.4	184.0	447.7	122.0	66.3	5.0	73.6	209.1	52.6	71.4	<0.05	-
K^+ (mg/L)	0.5	3.3	13.0	3.0	90.1	0.5	2.4	6.3	1.5	63.3	<0.05	12
Na^+ (mg/L)	1.1	24.4	101.3	28.4	116.3	1.5	54.6	207.2	56.6	103.5	<0.05	200
FeT (mg/L)	<DL	0.7	13.3	2.3	309.2	<DL	0.4	9.5	1.6	361.5	0.1	0.3
NH_4^+(mg/L)	<DL	0.0	0.7	0.1	248.7	<DL	<DL	<DL	<DL	<DL	0.3	1.5
NO_3^-(mg/L)	0.6	40.3	213.2	51.7	128.3	0.2	12.5	117.7	24.1	193.3	<0.05	50
NO_2^-(mg/L)	<DL	0.0	0.6	0.1	199.2	<DL	0.0	0.2	0.0	115.6	<0.05	3
Cl^- (mg/L)	3.9	48.6	245.0	37.7	77.5	7.1	27.2	61.1	12.0	44.3	<0.05	250
SO_4^2(mg/L)	<DL	16.3	115.8	24.7	152.2	0.5	9.5	56.0	12.8	134.9	0.8	250
PI(mg O_2/L)	0.3	0.5	3.9	0.6	119.1	<DL	0.6	2.5	0.4	70.5	<0.05	5

The dominance of major anions and cations is in the order of HCO_3^- > Cl^-> SO_4^{2-} > NO_3^- and Na^+> Mg^{2+} >

Ca^{2+} > K^+ in tap water, Cl^-> HCO_3^- > NO_3^- > SO_4^{2-} and Mg^{2+} > Na^+> Ca^{2+} > K^+ for surface water in the end of the rainy season, Cl^-> HCO_3^- > NO_3^- > SO_4^{2-} and Na^+ > Ca^{2+} > K^+ > Mg^{2+} for surface water in dry season, HCO_3^- > Cl^- > NO_3^- > SO_4^{2-} and Mg^{2+} > Na^+> Ca^{2+} > K^+ for groundwater in the end of the rainy season and HCO_3^- > Cl^- > NO_3^- > SO_4^{2-} and Na^+> Ca^{2+} > Mg^{2+} > K^+ for groundwater in dry season. Since tap water results from surface water treatment, differences in ion dominance between the two water types may be due to the use of aluminum sulfate salts for surface water clarification and sodium carbonate salts for water softening. Consequently, tap water gets enriched with Na^+ and SO_4^{2-} compared to surface water. Seasonal variation in ion dominance in surface water and groundwater suggests the control of season-driven changes in terrestrial hydrological system components, such as runoff and infiltration, as well as spatiotemporal variation in human-land interactions on water resource quality. These variations are evidenced by the high coefficient of variation values, except for pH and temperature.

3.2 Multivariate statistical

3.2.1 Correlation matrix

The correlation matrix (Fig 2), interpreted using the significance threshold ($p < 0.05$), on the basis that only the strongest coefficients correspond to meaningful relationships. Significant positive correlations among EC, TDS, Na^+, Mg^{2+}, Ca^{2+}, SO_4^{2-}, HCO_3^-, and total hardness indicate a dominant natural control through water-rock interactions and mineralization from silicate and carbonate-sulfate minerals. Cl^- showed significant correlation with ions such as NO_3^- and major cations, suggesting similar sources or concomitant input from anthropogenic sources that magnify water mineralization (Sodomon et al., 2025). NH_4^+, NO_2^-, and PI are positively and significantly correlated. These parameters may result from the decomposition of organic matter, including household garbage, vegetation, and animal or human dejections. They are negatively correlated with most ions, suggesting that anthropogenic degradation occurs episodically, mainly during conditions that favor intermittent leaching and runoff. Therefore, there is redox-controlled species mobilization.

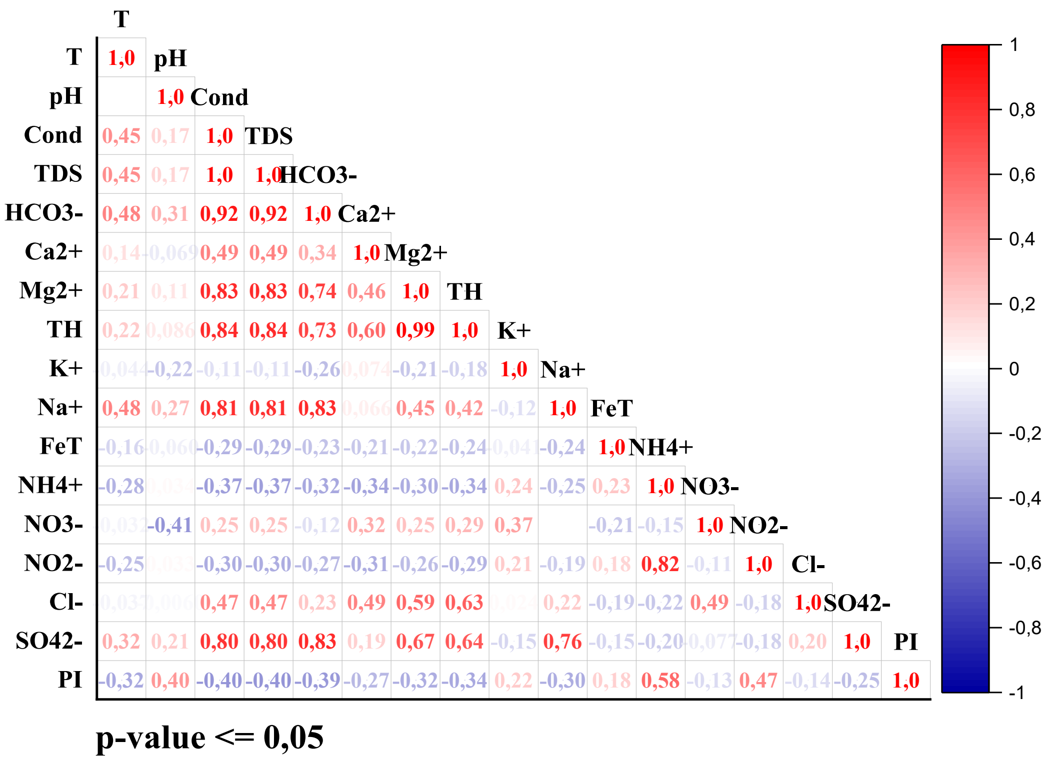

Fig 2: Pearson correlation matrix

3.2.2 Principal Component Analysis (PCA)

Table 8 presents the correlations between the original variables and the first five principal components,

showing the strength and direction of each parameter's contribution. The five retained components explain more than 80.60 % of the total variance, ensuring a robust representation of the dataset. PC1 (41.80%) is strongly controlled by EC, TDS, total hardness, and major ions (Ca^{2+}, Mg^{2+}, HCO_3^-, SO_4^{2-}, Na^+), reflecting a dominant natural mineralization gradient related to geological processes (ABV-OMM-GWP, 2016). PI, FeT, NH_4^+ , and NO_2^- load negatively and weakly on this axis, indicating a contrast with anthropogenic inputs from domestic wastewater, agriculture, or urban runoff (Akpataku et al., 2021; Mallya and Rwiza, 2021; Toi Bissang et al., 2023). PC2 (13.81%) opposed pH and NO_3^- loadings, defining a secondary gradient linked to redox conditions, acidification, and diffuse nitrogen enrichment (Hamma et al., 2024). PC3 (11.24%) groups PI, NH_4^+, and NO_2^-, suggesting organic contamination and microbial nitrogen transformations, and PC4 (7.72%) correlated with K^+. PC5 (6.03%) highlights FeT loading positively with pH and PI, which load negatively on this component, indicating antagonism between localized metal inputs and pH and episodic organic matter inputs. Overall, the PCA reveals three major gradients controlling water quality: natural mineralization, nitrogen enrichment from human activities, and localized physicochemical equilibrium conditions. These patterns underscore the system's spatial heterogeneity and the need for targeted, site-specific monitoring.

Table 8: PCA loadings and explained variance

	PC1	PC2	PC3	PC4	PC5
T	0.174	0.114	-0.233	0.439	-0.061
pH	0.052	0.421	0.107	-0.352	-0.496
Cond	0.364	0.054	0.102	0.095	0.016
TDS	0.364	0.054	0.102	0.095	0.016
HCO3-	0.337	0.247	-0.012	0.054	0.045
Ca2+	0.201	-0.303	0.097	-0.172	-0.084
Mg2+	0.325	-0.036	0.182	-0.207	0.171
TH	0.330	-0.089	0.182	-0.219	0.139
K+	-0.074	-0.219	0.310	0.494	-0.237
Na+	0.280	0.262	-0.010	0.293	-0.072
FeT	-0.129	0.108	0.011	-0.139	0.656
NH4+	-0.194	0.215	0.469	0.146	0.193
NO3-	0.084	-0.487	0.237	0.195	-0.050
NO2-	-0.169	0.202	0.463	0.178	0.214
Cl-	0.195	-0.291	0.289	-0.262	-0.040
SO42-	0.293	0.253	0.075	0.100	0.136
PI	-0.189	0.203	0.401	-0.155	-0.306

Eigenvalue	7.10534	2.3485	1.91129	1.31314	1.02539
% of Variance	41.80%	13.81%	11.24%	7.72%	6.03%
% of cumulative variance	41.80%	55.61%	66.85%	74.57%	80.60%

3.3 Hydrogeochemical facies

Piper diagrams (Fig 3) reveal hydrochemical contrasts between surface waters and waters in our study

area (Piper, 1944). Surface waters are mainly located in the Ca-Mg-Cl and Na-Cl fields, indicating a predominance of alkaline-earth cations and chloride associated with secondary soil salts and water-rock interaction pathways (Akpataku et al., 2019; Tshanga et al., 2025). A few samples show a slight deviation toward Ca-Mg and HCO_3 influences, suggesting a minor contribution. In contrast, groundwater samples show a wider distribution, with several falling within the mixed Ca-Mg-HCO_3, Na-HCO_3, Mg-Cl, and Ca-Mg-Cl facies. However, in the upper Oti sub-basin, within the Volta basin in Togo, Ca-Mg-HCO_3 and Na-HCO_3 are the dominant hydrochemical facies identified (Akakpo et al., 2025). Hydrochemical facies patterns reflect various geochemical evolution trends. However, the pollution characteristics of some samples suggest additional inputs consistent with agricultural or sewage contamination. Overall, the Piper diagrams indicate that surface waters and groundwater are mainly controlled by silicate and carbonate lithology, which dominate in the study area (Ani et al., 2025; Loh et al., 2012), and are shaped by geogenic-anthropogenic interactions.

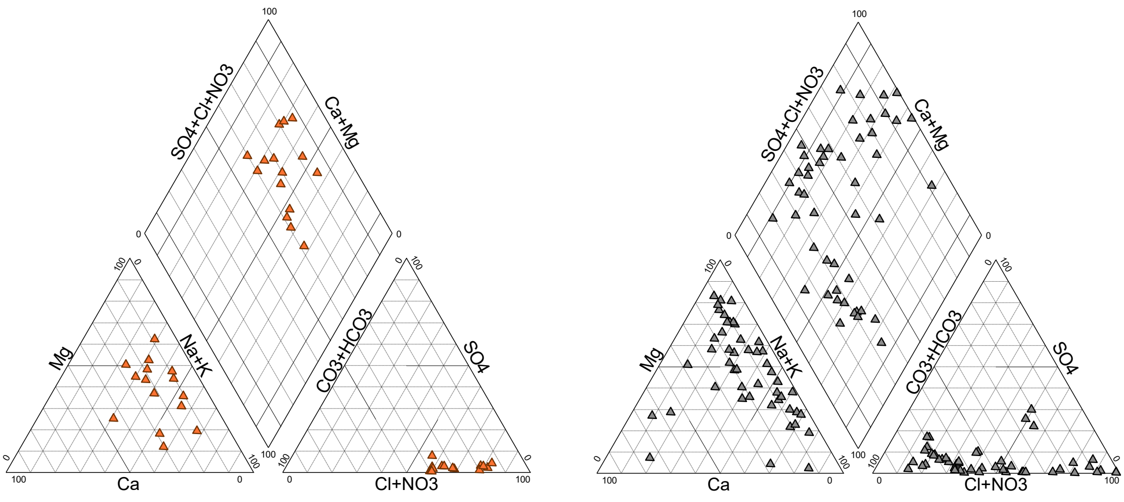

Surface Water　　　　Groundwater

Fig 3 : Piper diagram of surface water and groundwater

3.4 Gibbs diagram

Gibbs diagrams were used to identify the major mechanisms controlling the chemical composition of

water during the wet and dry seasons (Fig 4) (Gibbs, 1970). The ratios $Na^+/(Na^+ + Ca^{2+})$ and $Cl^-/(Cl^- + HCO_3^-)$ were plotted against Total Dissolved Solids (TDS). Fig 4 shows that most samples fall within the rock-weathering dominance field, indicating that the water's chemical composition is primarily controlled by interactions with the geological formations through which it flows. This distribution suggests that mineral dissolution is the primary source of dissolved ions in the study area's waters (Gao et al., 2019). The similar distribution observed during both the wet and dry seasons suggests that the hydrogeochemical mechanisms controlling water quality remain relatively stable throughout the hydrological cycle. Therefore, the Gibbs diagrams indicate that rock weathering is the dominant process controlling the chemical composition of waters in the Volta Basin, whereas evaporation exerts only a secondary influence (Mohamed et al., 2022).

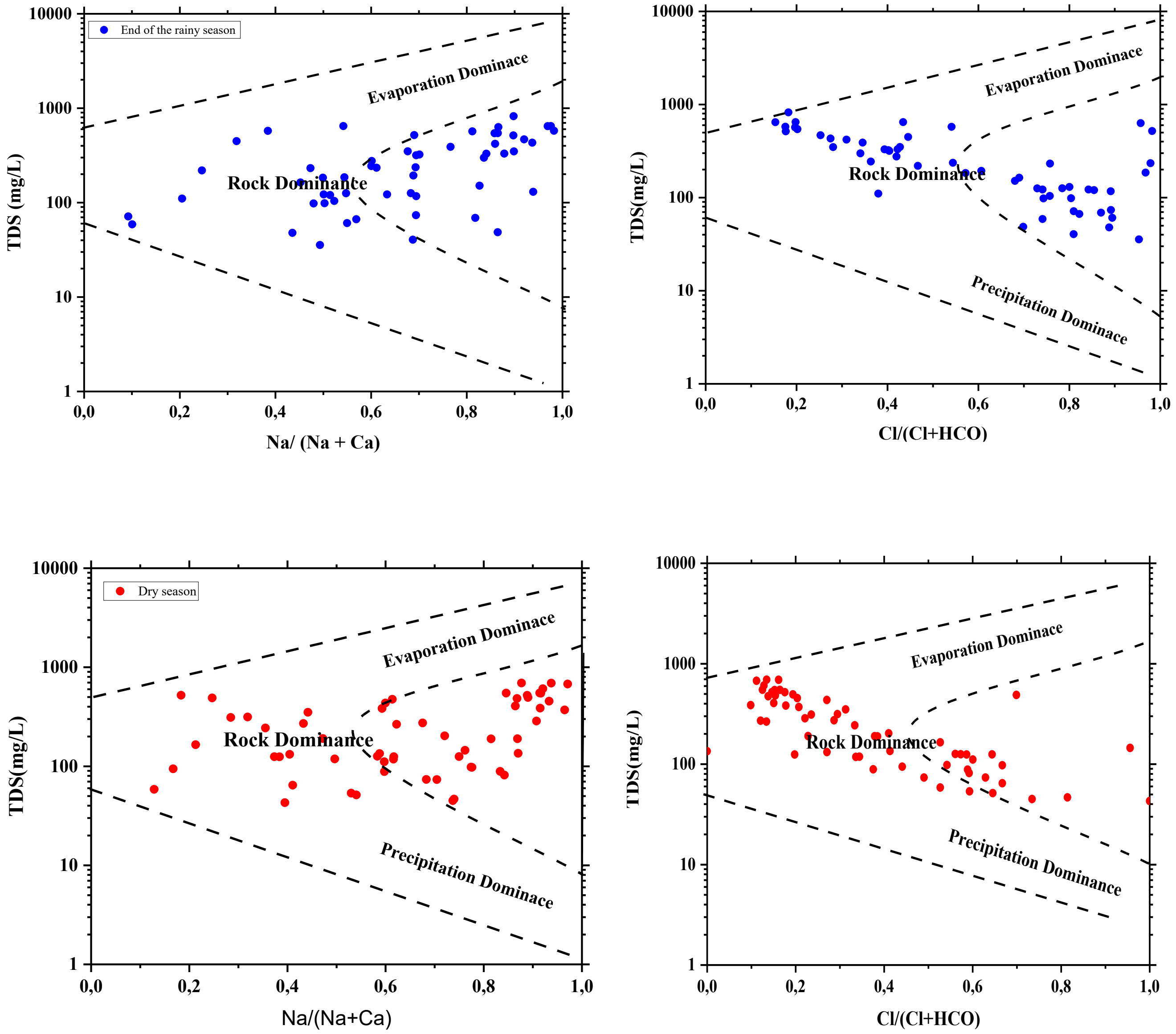

Fig 4: Gibbs diagram for the samples

3.5 Water chemistry controls

The chemical composition of water resources in the Togolese Volta Basin is examined. Anthropogenic

impacts on geochemical processes associated with water-rock interaction, including the dissolution of carbonate and silicate minerals, evaporite dissolution, and ion exchange, were analyzed using bivariate ionic diagrams (Appelo and Postma, 2010; Chidambaram et al., 2018).

The Na^+ *vs* Cl^- plot is used to assess the control of evaporitic or saline environments on both ions (Aweda et al., 2023). Fig 5a shows that sodium is not associated with chloride, ruling out the effect of evaporite salts, in line with the dominance of silicate rock in the study. High excesses of sodium over chloride suggest that it originates mainly from silicate minerals through water-rock interaction processes. At the seasonal scale, chloride may have a minor anthropogenic origin during the rainy season (Kitessa et al., 2024). The $Na^+ + K^+$ *vs* $Cl^- + SO_4^{2-}$ plot (Fig 5g) also shows that all points lie above the equivalence line, indicating an excess of $Na^+ + K^+$. This supports that alkaline cations do not originate from the dissolution of evaporitic minerals such as NaCl or Na_2SO_4. Instead, their origin would be predominantly linked to silicate weathering and ion-exchange processes (Wagh et al., 2025).

A Total Cations vs HCO_3^- diagram is used to assess the control exerted by carbonate minerals. Fig 5b shows that all samples plot above the equivalence line, indicating an excess of cations relative to bicarbonates. At the end of the rainy season, waters exhibit higher mineralization, reflecting enhanced mineral dissolution. In contrast, during the dry season, values are lower but still above the line, confirming that bicarbonates do not control mineralization. The $Ca^{2+} + Mg^{2+}$ *vs* $SO_4^{2-} + HCO_3^-$ diagram (Fig 5c) shows that most points, particularly during the wet season, plot above the 1:1 equivalence line, indicating an excess of $Ca^{2+} + Mg^{2+}$. This suggests that samples plotting above the line (end of the rainy season) and those below it (dry season) both reflect the seasonal control on geochemical processes of alkaline earth release in the basin's waters (Tay, 2021). In addition, the $Ca^{2+} + Mg^{2+}$ *vs* HCO_3^- (Fig 5d) plot further confirms that most samples lie above the equivalence line, indicating an excess of alkaline-earth cations relative to bicarbonates. This configuration shows that carbonate mineralization and dissolution are not prominent. At the end of the rainy season, higher Ca^{2+} and Mg^{2+} concentrations reflect an active hydrogeochemical regime driven by recharge. During the dry season, lower, more equilibrium-oriented values indicate less mineralized waters and a more stable hydrochemical regime.

The Total Cations *vs* $Ca^{2+} + Mg^{2+}$ (Fig 5e) plot shows that samples from the end of the rainy season exhibit strong mineralization and plot well above the equivalence line, indicating a significant contribution from other cations, particularly Na^+ and K^+. During the dry season, points lie closer to the line, suggesting that Ca^{2+} and Mg^{2+} dominate mineralization. Moreover, in the Total Cations *vs* $Na^+ + K^+$ plot (Fig 5f), most samples lie well above the equivalence line, demonstrating that total cations greatly exceed the contribution of $Na^+ + K^+$ alone. This pattern reflects silicate weathering and ion-exchange processes as key sources of cations (Aweda et al., 2023; Rai et al., 2023). The Na^+/Ca^{2+} plot (Fig 5h) shows a clear dominance of sodium over calcium, a trend that is particularly pronounced at the end of the rainy season. This confirms that Na^+ mainly originates from silicate weathering and ion-exchange processes. At the same time, Ca^{2+} remains relatively low, especially during the dry season, when waters are less mineralized under equilibrium-oriented conditions.

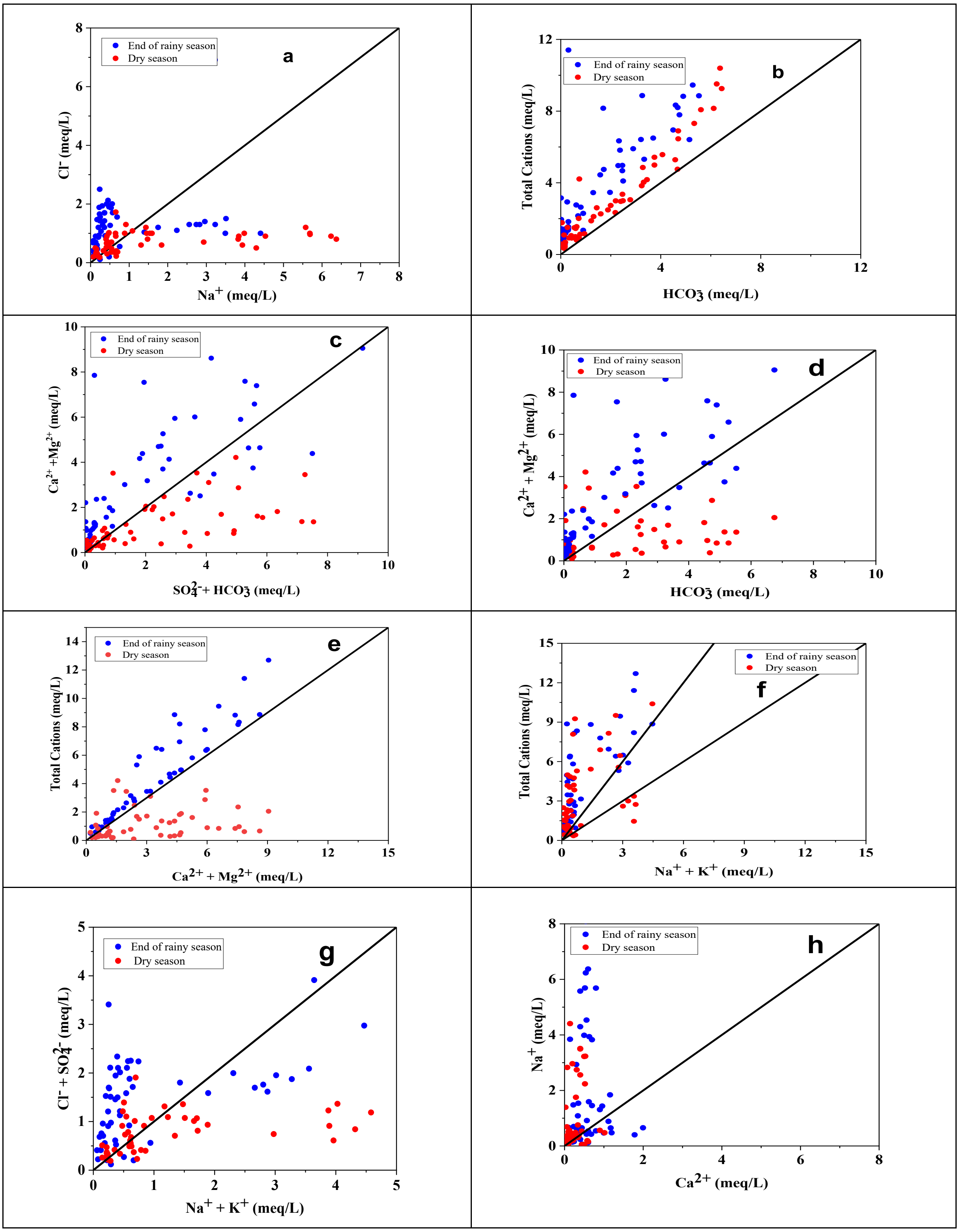

Fig 5: Bivariate plots

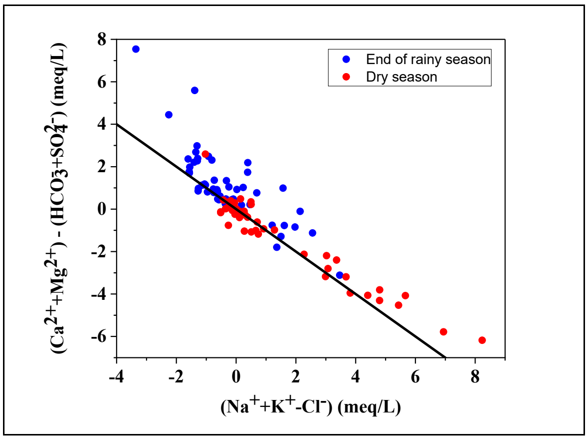

Fig 6 : Bivariate plot of ($Ca^{2+} + Mg^{2+}$) - ($HCO_3^- + SO_4^{2-}$) Vs ($Na^+ + K^+ - Cl^-$)

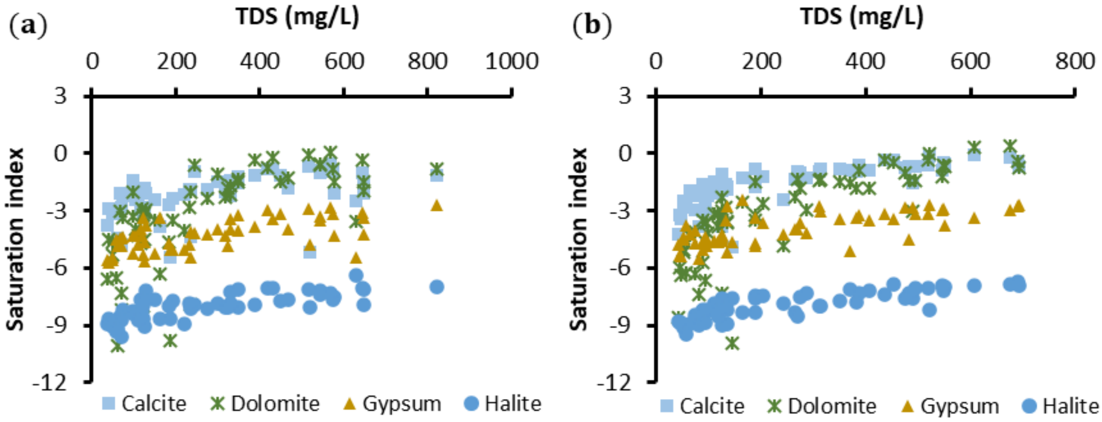

Fig 7: Saturation index of selected minerals (a) end of the rainy season and (b) dry season

The cross-plot (Fig 6) of ($Ca^{2+} + Mg^{2+}$) - ($HCO_3^- + SO_4^{2-}$) *vs* ($Na^+ + K^+ - Cl^-$) clearly highlights the ion-exchange processes that govern the chemical composition of the basin's waters. Most notably, most data points align along the 1:-1 trend (y = -x), indicating an ionic balance dominated by exchanges between alkaline cations (Na^+, K^+) and alkaline-earth cations (Ca^{2+}, Mg^{2+}) (Rai et al., 2023). Furthermore, seasonal differences are clearly evident. At the end of the rainy season, the more scattered values suggest an influence by processes driven by increased aquifer recharge, solute input, and contamination (Akpataku et al., 2019). Conversely, during the dry season, points are closer to and more evenly distributed along the exchange line, reflecting a more stable hydrochemical regime.

The saturation indices of calcite, dolomite, gypsum, and halite (Fig 7) indicate that all samples are undersaturated with respect to these minerals, suggesting an early stage of hydrochemical evolution of water resources in the study area. The variation in saturation index with TDS showed less regular evolution at the end of the rainy season than in the dry season, probably because recharge processes during the rainy season can induce thermodynamic disequilibrium. Overall, the basin's hydrochemistry results from a combination of natural processes, with the rainy season playing a key role in replenishing and enriching the water with dissolved ions. In contrast, the dry season favors a more stable, less concentrated, equilibrium-oriented chemical composition of water resources in the study area.

3.6 Drinking Water Suitability

Table 9 summarizes the Water Quality Index classes of surface water, tap water, and groundwater during the dry and rainy seasons.

Table 9 : Seasonal variation of Water Quality Index (WQI)

		Percentage of water samples as per WQI classes				
Seasons	Type of water	<25	25-50	50-75	75-100	>100
End of the rainy season	Surface water	20	0	10	0	70
	Tap water	50	25	0	25	0
	Groundwater	55	12	5	7	21
Dry season	Surface water	13	20	0	20	47
	Tap water	60	20	20	0	0
	Groundwater	64	13	10	3	10

During the dry season, surface water shows a mean WQI of about 197.7, indicating poor quality, with some sites reaching values above 440 and therefore classified as very poor or unfit for human consumption. About 33 % fell in the excellent category, while 20 % and 47 % fell in the very poor and unsuitable categories, respectively. In contrast, tap water samples (80 %) maintained excellent to good quality, whereas 20 % were of poor quality. Their mean value of 20.98 suggests that throughout the dry season, Tap water is safely within the acceptable range. Groundwater quality is highly variable during the dry season, with a mean WQI of 106.45. About 77 % fall into excellent to good water quality, 13 % into poor water quality, and 10 % into the unsuitable for drinking purposes category. These results highlight the deterioration of surface water compared to other water sources. During the rainy season, surface water quality further deteriorates, with a mean WQI of 394.7 and 70% of samples in the unsuitable category, indicating strong degradation. Tap water continues to exhibit good, stable quality (mean = 34.21), remaining reliably potable for 75% of samples, while 25% fell into the very poor category. Groundwater again shows considerable variability, with a mean WQI of 179.13, 67% falling into the excellent and good categories, and 21% into the unsuitable for drinking range, indicating that few groundwater sources become unsuitable for drinking during the wet season.

These quality indices have significantly higher values, likely due to higher iron content, than those reported in the watershed under similar conditions (Aher et al., 2016; Mammeri et al., 2023). Overall, tap water is the only consistently safe source in both seasons, while surface water and many groundwater sources are of very poor to unsuitable quality, especially during the rainy season. The greater deterioration of surface water is expected, as it results from surface runoff and is more vulnerable to surface contamination than groundwater. Assuming an efficient water treatment plant, poor Tap water quality may result from drinking water distribution systems that develop microbiochemical environments over decades, even under regular or intermittent service, along with pipe leakage and soil-water interactions (Fang et al., 2023; Shakya et al., 2022). These lead to pipe scaling and the release of elements such as Fe, Mn, and even toxic elements such as Pb, and can significantly impact water quality at customers' taps. The presence of these elements may explain the relatively high permanganate oxidability index PI. The situation in the study area calls for systematic maintenance of the water distribution network and service lines, as well as regular monitoring of tap water quality across a range of chemical variables.

3.7 Suitability of Water for Irrigation

The sodium adsorption ratio (SAR) is a key indicator of the risk associated with sodium in irrigation

water. SAR values (Table 10) indicate that at the end of the rainy season, 100% of sampling points have values < 10, placing them in the ‘excellent’ category for irrigation suitability. The same tendency is observed in surface water during the dry season. The percentage of sodium (Na%) is a key parameter used to assess the potential risks associated with excess sodium in irrigation water. High %Na values indicate an increased risk of soil sodium accumulation, which can lead to soil particle dispersion, reduced soil permeability, and decreased aeration. The %Na index has been used to distinguish five water quality classes (Kawo and Karuppannan, 2018). The %Na index shows high variability between sampling points. At the end of the rainy season, 80% of surface water samples fall into the “excellent” category (< 20) and 20% into the “good” category (20-40), both of which are suitable for irrigation (Barik and Pattanayak, 2019). For groundwater, 54% is excellent (<20), 29% is good (20-40), 15% is average (40-60), and 2% is poor (60-80). During the dry season, this distribution is reversed: 53% of groundwater samples fall into the ‘unsuitable’ category (80-100), and 27% of surface water is classified as ‘poor’ (60-80), indicating a susceptibility to soil sodium enrichment under low flow conditions. This high Na concentration ultimately impairs water infiltration and root development, thereby limiting crop productivity (Kadjangaba et al., 2023; Kumar et al., 2022). Na% is therefore essential for assessing the immediate and long-term suitability of water for sustainable irrigation.

The Kelly ratio (KR) used in this study is an important indicator of irrigation water quality. KR values, which are generally above 1 during both seasons, further confirm a low risk of sodicity and overall compatibility with irrigation (Kadjangaba et al., 2023; Kumar et al., 2024). High magnesium concentrations can compromise crop productivity, as this element, when present in excess, contributes more to increasing soil alkalinity than

calcium. For this reason, it is essential to assess magnesium in irrigation water using the magnesium hazard index (MH) (Kumar et al., 2024). For the MH, at the end of the rainy season, almost all sampling points have values > 50, corresponding to unsuitable irrigation water, except for two groundwater points. During the dry season, 40% of surface water samples and 68% of groundwater samples also exceeded 50, indicating less favorable irrigation water quality than during the wet season.

RSC is used to determine the potential impact of irrigation water on soil structure, permeability, and productivity. It plays an important role in areas with high concentrations of carbonates and bicarbonates. RSC values are classified as <1.25, 1.25-2.5, and >2.5 as suitable, questionable/poor, and unsuitable, respectively. The RSC index shows that 98% of points at the end of the rainy season have values < 1.25, which corresponds to ‘good’ to ‘excellent’ quality for irrigation. During the dry season, only 54% of surface water and 10% of groundwater samples fall into this category. In addition, 13% of surface water and 16% of groundwater samples during the dry season were of poor quality (1.25-2.5), and 33% of surface water and 74% of groundwater were unsuitable (> 2.5), indicating significant carbonate accumulation during the dry period.

The presence of salts in irrigation water, such as Na^+, Ca^{2+}, Mg^{2+} , and HCO_3^-, can affect soil permeability. To assess this impact, the quality of irrigation water is classified using the permeability index (PI). In terms of PI, at the end of the rainy season, 90% of surface water falls into the ‘good’ category (25-75) and 10% into the ‘excellent’ category (> 75). For groundwater, 7% is unsuitable (<25), 73% is good, and 20% is excellent. During the dry season, 100% of surface water samples are excellent, while 95% of groundwater samples are excellent and 5% are good. Finally, the potential salinity index (PS) shows that all sampling points, except one, have values < 3, placing them in the “excellent” category for salinity risk from irrigation when water evaporates or is absorbed by plants (Mohanavelu et al., 2021).

Table 10 : Seasonal variation of irrigation suitability indices

Percentage of water samples as per irrigation purpose classes					
	Rang	End of the rainy season		Dry season	
		Surface water	Groundwater water	Surface water	Groundwater water
SAR	<10	100	100	100	95
	6-18	0	0	0	5
	18-26	0	0	0	0
	>26	0	0	0	0
%Na	<20%	80	54	0	16
	20-40%	20	29	20	13
	40-60%	0	15	53	0
	60-80%	0	2	27	18
	80-100%	0	0	0	53
RSC	<1.25	100	98	54	10
	1.25-2.5	0	2	13	16
	>2.5	0	0	33	74
KR	<1	0	0	0	0
	>1	100	100	100	100
MH	<50	0	2	60	32
	>50	100	98	40	68
PI	<25	0	7	0	0
	25-75	90	73	0	5
	>75	10	20	100	95
PS	<3	100	98	100	100
	3-5	0	0	0	0
	>5	0	2	0	0

3.8 Suitability of water for industrial use

The assessment of the corrosive and scaling potential of water using saturation and stability indices (Table 11) highlights the aptitude of water resources for industrial use during the two seasons considered in this study. The Langelier saturation index shows negative values. These negative values (LSI < 0) were observed in all samples except for one sampling point. It reflects calcium carbonate undersaturation, indicating a low capacity of the water to form a protective $CaCO_3$ film on metal surfaces, which promotes corrosion of metal installations (Kumar et al., 2024). This is explained by low mineralization, characterized by low alkalinity and low hardness content (Lodha et al., 2023).

Table 11: Seasonal variation of industrial stability indices

Percentage of water samples as per industrial purpose classes					
	Rang	End of the rainy season		Dry season	
		Surface water	Groundwater water	Surface water	Groundwater water
LSI	<0	100	97	100	100
	0±0.5	0	3	0	0
	>0.5	0	0	0	0
PSI	<5	0	0	0	0
	5-6	0	45	0	0
	>8	100	55	100	100
RSI	<6	0	0	0	0
	>7	100	100	100	100
LI	<0.8	30	81	0	5
	0.8-1.2	0	2	0	13
	>1.2	70	17	100	82

The Ryznar Stability Index (RSI) shows values above 7 (RSI > 7) for all samples during the two campaigns. This translates into a high propensity for calcium carbonate dissolution, to the detriment of deposition (Dougna et al., 2024). High RSI values are typically associated with aggressive waters, which can accelerate the corrosion of concrete and even metallic materials, particularly when the pH and alkalinity are insufficient to stabilize the carbonate system. The concordance between the LSI and RSI results thus reinforces the reliability of the corrosion diagnosis established for the waters in the study area. At the end of the rainy season, all water samples had PSI values above 8, indicating a marked tendency towards corrosion. This situation is attributed to the dilution of alkali and alkaline earth ions by rainfall, leading to a decrease in water alkalinity and chemical stability. In the dry season, although the majority of sampling points (68%) maintain PSI values > 8, reflecting a predominantly corrosive behavior, a significant proportion of samples (32%) show values between 5 and 7. This trend suggests a slight tendency towards scaling at certain sites, probably linked to increased water mineralization, higher solute concentrations, and longer water-rock interactions in the aquifer systems.

Furthermore, the Larson-Skold index (LI) highlights the influence of anions, particularly chlorides and

sulfates, on the stability of the protective calcium carbonate film. At the end of the rainy season, the majority of groundwater samples (81%) are of good quality (LI < 0.8), indicating a low impact of aggressive anions on corrosion. However, 17% of samples have LI values above 1.2, indicating a high risk of corrosion, probably linked to anthropogenic inputs or the dissolution of geological formations rich in soluble salts. During the dry season, the situation deteriorates, with 100% of surface water and 82% of groundwater showing LI values > 1.2. This increase in corrosive potential during low-water periods can be explained by the higher concentrations of chloride and sulfate ions resulting from evaporation, reduced flow rates, and intensified anthropogenic pressures. All these LSI, RSI, PSI, and LI indices highlight the corrosive nature of the water in our study area, posing a potential risk to infrastructure durability.

3.9 Sustainable management of water resources

Based on the hydrochemical patterns, water quality indices, and statistical analyses obtained in this study,

several actions are recommended to ensure the sustainable management of water resources in the Togolese part of the Volta Basin:

i. Strengthen monitoring of critical water quality parameters: Seasonal fluctuations and episodes of nitrate, iron, and chloride contamination highlight the need for continuous monitoring of nitrates, iron, chlorides, sodium, magnesium, and sulfate, especially during the rainy season.
ii. Protect groundwater recharge zones: During the rainy season, increased infiltration can increase mineralization and transport pollutants toward aquifers. It is important to control anthropogenic activities near recharge areas; avoid activities that could pollute them; and avoid dumping domestic waste or wastewater into infiltration zones.
iii. Secure and maintain drinking-water infrastructures: Since tap water is the only consistently safe source, it is important to expand access to piped water networks and secure boreholes.

- Establish community-based water governance: Sustainable management requires local water committees involving farmers, households, and authorities; awareness campaigns on pollution risks and safe water use; transparent sharing of water-quality data with communities; and strengthened collaboration with the Volta Basin Authority (VBA) to ensure coordinated, basin-wide water management.

4. Conclusion

This study provides a comprehensive assessment of water quality in the Togolese sector of the Volta Basin.

It highlights a hydrochemical system strongly influenced by seasonal dynamics and local geological conditions. During the rainy season, groundwater becomes significantly more mineralized due to enhanced infiltration and solute transfer from the land surface or the vadose zone. In contrast, surface waters experience marked dilution, even as they receive increased nutrient and iron inputs from agricultural runoff and domestic discharges. These patterns reveal a high vulnerability of both aquifers and surface waters to contamination. The Water Quality Index shows that only tap water consistently meets drinking-water standards. A few groundwater and surface water samples exceed recommended limits for nitrates and iron, especially during the wet season. Despite this, most waters remain generally suitable for irrigation, although attention is required regarding sodium, magnesium, and residual salinity, which may affect soil structure and crop productivity. Industrial stability indices further indicate variable risks of corrosion and scaling, posing challenges to the long-term integrity of water supply hydraulic infrastructure. Water quality in the basin is controlled by a combination of natural mineralization processes, such as the weathering of carbonate and silicate minerals, and ion exchange, as well as anthropogenic inputs from agriculture and domestic activities. These results highlight the need to implement integrated water resource management strategies, including strengthening monitoring of sensitive parameters, such as microbiological indicators; protecting recharge zones; reducing pollution sources; and developing public awareness initiatives. Such measures are essential to ensure the sustainable and safe use of water resources throughout the Volta River Basin.

Declarations

Funding

This research was financially supported by the World Bank (WB) and the French Development Agency (AFD) through the C2EA at the University of Abomey-Calavi, Benin.

Conflict of interest

The authors declare that they have no known competing financial interests or personal relationships that could have influenced the work reported in this paper.

Acknowledgments

The authors thank the World Bank (WB) and the French Development Agency (AFD) for supporting this work through the African Centre of Excellence for Water and Sanitation (C2EA) at the University of Abomey-Calavi.

References

ABV-OMM-GWP, 2016. Préparation de Projets de Mise en Œuvre de la Gestion Intégrée des Crues - GIC dans le bassin de la Volta et ses six pays riverains (Bénin, Burkina Faso, Côte d'Ivoire, Ghana, Mali et Togo).

Affaton, P., 1987. Le bassin des Volta (Afrique de l'Ouest) : une marge passive, d'âge Protérozoïque Supérieur, Tectonitisée au Panafricain (600 ± 50 Ma). Thèse de Doctorat d'Etat de l'Université d'Aix-Marseille II, France.

Aher, D.N., Kele, Malwade K, Shelke, M.D., 2016. Lake Water Quality Indexing To Identify Suitable Sites For Household Utility: A Case Study Jambhulwadi Lake;Pune(MS). Int J. Eng. Res. Appl. 6, 6–21.

Ahmed, S., Sultan, M.W., Alam, M., Hussain, A., Qureshi, F., Khurshid, S., 2021. Evaluation of corrosive behaviour and scaling potential of shallow water aquifer using corrosion indices and geospatial approaches in regions of the Yamuna river basin. J. King Saud Univ. - Sci. 33, 101237. https://doi.org/10.1016/j.jksus.2020.101237

Aju, C.D., L., A., P, M., Mani Christy, R., Reghunath, R., Gopinath, G., 2024. Emerging Nitrate Contamination in Groundwater: Changing Phase in a Fast-Growing State of India. Chemosphere 357, 141964. https://doi.org/10.1016/j.chemosphere.2024.141964

Akakpo, Y., Bleza, A., Boguido, G., Zouari, K., Trabelsi, R., 2025. Évaluation hydrogéochimique des aquifères du bassin des volta : cas du sous bassin de l'Oti supérieur au Togo. Afr. Sci. 26, 91–104.

Akhtar, N., Ishak, M.I.S., Ahmad, M.I., Umar, K., Md Yusuff, M.S., Anees, M.T., Qadir, A., Ali Almanasir, Y.K., 2021. Modification of the Water Quality Index (WQI) Process for Simple Calculation Using the Multi-Criteria Decision-Making (MCDM) Method: A Review. Water 13, 905.

https://doi.org/10.3390/w13070905

Akpaki, O., Oudja, B., Baba, G., 2019. Impact of mining and agricultural activities on water chemical quality of the volta bassin in Togo over 2015-2017. Durb. South Afr.

Akpataku, K.V., Gnazou, M.D.T., Agbefu Nomesi, Y.T., Nambo, P., Doni, K., Bawa, L.M., Djaneye-Boundjou, G., 2021. Assessment of hydrological factors affecting shallow groundwater chemistry in the most urbanized area of the coastal sedimentary basin of Togo, in: Proceedings of the International Association of Hydrological Sciences. Presented at the Hydrology of Large River Basins of Africa - 4th International Conference on the "'Hydrology of the Great Rivers of Africa,'" Copernicus GmbH, pp. 75–80. https://doi.org/10.5194/piahs-384-75-2021

Akpataku, K.V., Gnazou, M.D.T., Djanéyé-Boundjou, G., Bawa, L.M., Faye, S., 2020. Role of Natural and Anthropogenic Influence on the Salinization of Groundwater from Basement Aquifers in the Middle Part of Mono River Basin, Togo. J. Environ. Prot. 11, 1030–1051.

https://doi.org/10.4236/jep.2020.1112065

Akpataku, K.V., Halder, J., Rai, S.P., Bawa, L.M., Djaneye-Boundjou, G., Gnazou, D.-T.M., Faye, S., 2025a. Tracing nitrate sources and denitrification potential using chemical, multi-isotopic, and Bayesian mixing model approaches in the Plateaux Region of Togo, West Africa. J. Environ. Chem. Eng. 13, 117170. https://doi.org/10.1016/j.jece.2025.117170

Akpataku, K.V., Rai, S.P., Gnazou, M.D.-T., Tampo, L., Bawa, L.M., Djaneye-Boundjou, G., Faye, S., 2019. Hydrochemical and isotopic characterization of groundwater in the southeastern part of the Plateaux Region, Togo. Hydrol. Sci. J. 64, 983–1000. https://doi.org/10.1080/02626667.2019.1615067

Akpataku, K.V., Tchapo, K., Dougna, A.A., Ani, M., Sodomon, A.K., Mande, S.-L.A.-S., Bawa, L.M., Faye, S., 2025b. Hydrogeochemical Characteristics of Groundwater in the Prefecture of Bassar, Togo. Am. J. Chem. Eng. 12, 1–13. https://doi.org/10.11648/j.ajche.20251301.11

Ani, M., Jaunat, J., Marin, B., Barel, M., Gnandi, K., 2022. Long-Term Evolution of Rainfall and Its Consequences on Water Resources: Application to the Watershed of the Kara River (Northern Togo). Water 14, 1976. https://doi.org/10.3390/w14121976

Ani, M., Jaunat, J., Marin, B., Huneau, F., Gnandi, K., 2025a. Using archive hydrogeological data to enhance the hydrodynamic knowledge of hardrock aquifers in Western Africa. J. Afr. Earth Sci. 221, 105477. https://doi.org/10.1016/j.jafrearsci.2024.105477

Ani, M., Jaunat, J., Marin, B., Huneau, F., Gnandi, K., 2025b. Using archive hydrogeological data to enhance the hydrodynamic knowledge of hardrock aquifers in Western Africa. J. Afr. Earth Sci. 221, 105477. https://doi.org/10.1016/j.jafrearsci.2024.105477

Anornu, G., Gibrilla, A., Adomako, D., 2017. Tracking nitrate sources in groundwater and associated health risk for rural communities in the White Volta River basin of Ghana using isotopic approach (δ 15 N, δ 18 O NO 3 and 3 H). Sci. Total Environ. 603–604, 687–698.
https://doi.org/10.1016/j.scitotenv.2017.01.219

Appelo, C.A.J., Postma, D., 2010. Geochemistry, groundwater and pollution, 2nd ed., 5th corr. repr. ed. Taylor & Francis Group plc, Boca Raton.

Aweda, A.K., Jatau, B.S., Goki, N.G., 2023. Groundwater geochemistry and hydrochemical processes in the Egbako aquifer, Northern Bida Basin, Nigeria. RBRH 28, e31. https://doi.org/10.1590/2318-0331.282320230010

Ayeni, O.O., Oyegoke, S.O., Ndububa, O.I., Adetoro, A.E., 2023. Physico-chemical and bacteriological assessments of shallow well water samples during the dry and rainy seasons. Niger. J. Technol. Dev. 20, 43–52. https://doi.org/10.4314/njtd.v20i2.1291

Badjana, H.M., Renard, B., Helmschrot, J., Edjamé, K.S., Afouda, A., Wala, K., 2017. Bayesian trend analysis in annual rainfall total, duration and maximum in the Kara River basin (West Africa). J. Hydrol. Reg. Stud. 13, 255–273. https://doi.org/10.1016/j.ejrh.2017.08.009

Barik, R., Pattanayak, S.K., 2019. Assessment of groundwater quality for irrigation of green spaces in the Rourkela city of Odisha, India. Groundw. Sustain. Dev. 8, 428–438.
https://doi.org/10.1016/j.gsd.2019.01.005

Barry, B., Obuobie, E., Andreini, M., Andah, W., Pluquet, M., 2025. The Volta River basin: Comprehensive Assessment of Water Management in Agriculture: Comparative study of river basin development and management.

Bekri, M.H., El Hmaidi, A., Jaddi, H.J., Kasse, Z., Mati El Faleh, E.M.E.F., Essahlaoui, A., El Ouali, A., 2020. Utilisation Des Indices De Qualité Et De Pollution Organique Dans L'évaluation De La Qualité Physico-Chimique Des Eaux Superficielles Des Oueds Moulouya et Ansegmir (Haute Moulouya, NE Du Maroc). Eur. Sci. J. ESJ 16, 55. https://doi.org/10.19044/esj.2020.v16n27p55

Ben Moussa, A., Mzali, H., Elmejri, H., Bel Haj Salem, S., 2019. Apport des outils hydrogéochimiques à l'évaluation de la qualité et l'aptitude des eaux souterraines à l'irrigation : cas de la nappe phréatique de la basse vallée de Medjerda, Tunisie Nord-Orientale. Houille Blanche 105, 35–44. https://doi.org/10.1051/lhb/2019053

Block, S., Jessell, M., Aillères, L., Baratoux, L., Bruguier, O., Zeh, A., Bosch, D., Caby, R., Mensah, E., 2016. Lower crust exhumation during Paleoproterozoic (Eburnean) orogeny, NW Ghana, West African Craton: Interplay of coeval contractional deformation and extensional gravitational collapse. Precambrian Res. 274, 82–109. https://doi.org/10.1016/j.precamres.2015.10.014

Bordalo, A.A., Nilsumranchit, W., Chalermwat K, 2001. Water quality and uses of the Bangpakong River (Eastern Thailand) 1 , W 2 , K 3. Water Res. 35, 3635–3642. https://doi.org/10.1016/S0043-1354(01)00079-3

Burri, N.M., Weatherl, R., Moeck, C., SChirmer, M., 2019. A review of threats to groundwater quality in the anthropocene. Sci. Total Environ. 684, 136–154. https://doi.org/10.1016/j.scitotrnv.2019.05.236

Çadraku, H.S., Beqiraj, A., 2023. Assessment of water quality in Blinaja River Basin (Kosovo) using the Canadian Water Quality Index (WQI). J. Surv. Fish. Sci. 10, 29–47.

Chidambaram, S., Sarathidasan, J., Srinivasamoorthy, K., Thivya, C., Thilagavathi, R., Prasanna, M.V., Singaraja, C., Nepolian, M., 2018. Assessment of hydrogeochemical status of groundwater in a coastal region of Southeast coast of India. Appl. Water Sci. 8, 27. https://doi.org/10.1007/s13201-018-0649-2

Dehghani, M., Keshtgar, L., Davoodi, S., Shamsedini, N., Zaravar, F., 2019. Data on the trend of corrosivity and scale formation potential of Shiraz groundwater drinking water resources during 2001-2007. Data Brief 23. https://doi.org/10.1016/j.dib.2019.103736

Dougna, A.A., Kolani, J.M., Akpataku, K.V., Tchakala, I., Tampo, L., Seyf-Laye, A.-S.M., Bawa, M.L., 2024. Quality and Chlorine Demand of Private Raw Borehole Water in the City of Kara, Togo. Am. J. Appl. Chem. 12, 158–172. https://doi.org/10.11648/j.ajac.20241206.14

Eid, M.H., Elbagory, M., Tamma, A.A., Gad, M., Elsayed, S., Hussein, H., Moghanm, F.S., Omara, A.E.-D., Kovács, A., Péter, S., 2023. Evaluation of Groundwater Quality for Irrigation in Deep Aquifers Using Multiple Graphical and Indexing Approaches Supported with Machine Learning Models and GIS Techniques, Souf Valley, Algeria. Water 15, 182. https://doi.org/10.3390/w15010182

El Baba, M., Kayastha, P., Huysmans, M., De Smedt, F., 2020. Evaluation of the Groundwater Quality Using the Water Quality Index and Geostatistical Analysis in the Dier al-Balah Governorate, Gaza Strip, Palestine. Water 12, 262. https://doi.org/10.3390/w12010262

El Baroudi, H., Ouazzani, C., Moustaghfir, A., Er-Ramly, A., El Baroudi, Y., Dami, A., Balouch, L., 2024. Assessing the Corrosion and Scaling Potential of Drinking Water in Morocco Using Water Stability Indices. Ecol. Eng. Environ. Technol. 25, 130–139. https://doi.org/10.12912/27197050/175970

Fang, J., Dai, Z., Li, X., van der Hoek, J.P., Savic, D., Medema, G., van der Meer, W., Liu, G., 2023. Service-lines as major contributor to water quality deterioration at customer ends. Water Res. 241, 120143. https://doi.org/10.1016/j.watres.2023.120143

Gao, Z., Liu, J., Feng, J., Wang, M., Wu, G., 2019. Hydrogeochemical Characteristics and the Suitability of Groundwater in the Alluvial-Diluvial Plain of Southwest Shandong Province, China. Water 11. https://doi.org/10.3390/w11081577

Gebrechorkos, S.H., Pan, M., Lin, P., Anghileri, D., Forsythe, N., Pritchard, D.M.W., Fowler, H.J., Obuobie, E., Darko, D., Sheffield, J., 2022. Variability and changes in hydrological drought in the Volta Basin, West Africa. J. Hydrol. Reg. Stud. 42, 101143. https://doi.org/10.1016/j.ejrh.2022.101143

George-Williams, H.E.M., Hunt, D.V.L., Rogers, C.D.F., 2024. Sustainable Water Infrastructure: Visions and Options for Sub-Saharan Africa. Sustainability 16, 1592. https://doi.org/10.3390/su16041592

Gibbs, R.J., 1970. Mechanisms controlling world water chemistry. Science 170.

Giri, S., Tiwari, A.K., Mahato, M.K., Singh, A.K., 2025. Major ion chemistry and suitability of groundwater resources for different utilizations in mica mining areas, Jharkhand, India. Geochem. Trans. 26, 5. https://doi.org/10.1186/s12932-025-00099-x

Goumpoukini, B., Massabalo, A., Kamel, Z., Moctar, B.L., Gbandi, B., 2019. Analysis of Hydraulic Properties of Discontinuous Aquifers Basement of the Birimian Basin in Northern Togo. J. Sci. Eng. Res. 6, 90–101.

GWP, 2019. Volta River Basin: Building Climate Resilience of People and Ecosystems [WWW Document]. URL https://waterknowledgehub.org/case-study/volta-river-basin-building-climate-resilience-people-and-ecosystems? (accessed 11.19.25).

Hamma, B., Alodah, A., Bouaicha, F., Bekkouche, M.F., Barkat, A., Hussein, E.E., 2024. Hydrochemical assessment of groundwater using multivariate statistical methods and water quality indices (WQIs). Appl. Water Sci. 14, 33. https://doi.org/10.1007/s13201-023-02084-0

Huang, F., Wang, X., Lou, L., Zhou, Z., Wu, J., 2010. Spatial variation and source apportionment of water pollution in Qiantang River (China) using statistical techniques. Water Res. 44, 1562–1572. https://doi.org/10.1016/j.watres.2009.11.003

Kadjangaba, E., Bongo, D., Bandoumel, M.L., 2023. Adequacy of Water Use Resources for Drinking and Irrigation, Study Case of Sarh City, Capital of Moyen-Chari Province, CHAD. Open J. Mod. Hydrol. 13, 1–21. https://doi.org/10.4236/ojmh.2023.131001

Kawo, N.S., Karuppannan, S., 2018. Groundwater quality assessment using water quality index and GIS technique in Modjo River Basin, central Ethiopia. J. Afr. Earth Sci. 147, 300–311. https://doi.org/10.1016/j.jafrearsci.2018.06.034

Kitessa, W.M., Kebede, A.B., Tufa, F.G., Gudeta, B.G., Yenehun, A., Chelkeba, B., Debela, S.K., Feyessa, F.F., Walraevens, K., 2024. Hydrogeochemical Characterization and Processes Controlling Groundwater Chemistry of Complex Volcanic Rock of Jimma Area, Ethiopia. Water 16, 3470.
https://doi.org/10.3390/w16233470

Koukou-Tchamba, A., 2022. Intégration de la gestion des inondations et de la sécheresse et l'alerte précose pour l'adaptation au changement climatique dans le bassin de la Volta. Togo.

Kumar, R., Sharma, S., Prashant, M., 2024. Assessment of groundwater quality for drinking, irrigation and industrial purposes in Aik Watershed, Jammu and Kashmir, India. Discov. Geosci. 2, 58. https://doi.org/10.1007/s44288-024-00065-7

Kumar, S., Maurya, N.S., 2025. Analysis of heavy metal contamination in groundwater and associated probabilistic human health risk assessment using Monte Carlo simulation: A case study in Gaya, Bihar. J. Water Health 23, 630–647. https://doi.org/10.2166/wh.2025.348

Kumar, S., Singh, R., Maurya, N.S., 2022. Assessment of Corrosion Potential Based on Water Quality Index in the Distribution Network of Urban Patna, Bihar, India. Nat. Environ. Pollut. Technol. 21, 2117–2127. https://doi.org/10.46488/NEPT.2022.v21i05.008

Lachassagne, P., Dewandel, B., Wyns, R., 2021. Review: Hydrogeology of weathered crystalline/hard-rock aquifers—guidelines for the operational survey and management of their groundwater resources. Hydrogeol. J. 29, 2561–2594. https://doi.org/10.1007/s10040-021-02339-7

Lartsey, P., Ganyaglo, S., Adomako, D., Sakyi, P., Gibrilla, A., Barbecot, F., Lefebvre, K., Nsikanabasi, E., 2024. Tracing Nitrate Contamination Sources and Apportionment in North-Western Volta River Basin of Ghana Using a Multi-Isotopic Approach. Water. Air. Soil Pollut. 235, 123456789.
https://doi.org/10.1007/s11270-024-07418-5

Lodha, R., Sharma, Y., Surecha, O.P., Trivedi, A., Chaplot, H., Chaudhary, M., Choudhary, S., 2023. Scaling Potential and Corrosion Assessment through Langelier Saturation Index and Ryznar Stability Index of Under Ground Water in Udaipur, Rajasthan. IARJSET 10.
https://doi.org/10.17148/IARJSET.2023.10735

Loh, Y.S., Banoeng-Yakubo, B., Yidana, S.M., Asiedu, D., Akabzaa, T., Jørgensen, N.O., 2012. Hydrochemical Characterisation of Groundwater in Parts of the Volta Basin, Northern Ghana. Ghana Min. J. 13, 24–32.

Ma, X., Wang, L., Yang, H., Li, N., Gong, C., 2020. Spatiotemporal Analysis of Water Quality Using Multivariate Statistical Techniques and the Water Quality Identification Index for the Qinhuai River Basin, East China. Water 12, 2764. https://doi.org/10.3390/w12102764

Mahaqi, A., Moheghi, M.M., Mehiqi, M., Moheghy, M.A., 2018. Hydrogeochemical characteristics and groundwater quality assessment for drinking and irrigation purposes in the Mazar-i-Sharif city, North Afghanistan. Appl. Water Sci. 8, 133. https://doi.org/10.1007/s13201-018-0768-9

Mallya, C.L., Rwiza, M.J., 2021. Influence of land use change on nitrate sources and pollutant enrichment in surface and groundwater of a growing urban area in Tanzania. Environ. Earth Sci. 80, 111. https://doi.org/10.1007/s12665-021-09386-z

Mammeri, A., Tiri, A., Belkhiri, L., Salhi, H., Brella, D., Lakouas, E., Tahraoui, H., Amrane, A., Mouni, L., 2023. Assessment of Surface Water Quality Using Water Quality Index and Discriminant Analysis Method. Water 13, 680. https://doi.org/10.3390/w15040680

Manu, E., De Lucia, M., Kühn, M., 2023. Hydrochemical Characterization of Surface Water and Groundwater in the Crystalline Basement Aquifer System in the Pra Basin (Ghana). Water 15, 1325. https://doi.org/10.3390/w15071325

McClain, M.E., 2013. Balancing Water Resources Development and Environmental Sustainability in Africa: A Review of Recent Research Findings and Applications. AMBIO 42, 549–565. https://doi.org/10.1007/s13280-012-0359-1

Mohamed, A., Asmoay, A., Alshehri, F., Abdelrady, A., Othman, A., 2022. Hydro-Geochemical Applications and Multivariate Analysis to Assess the Water–Rock Interaction in Arid Environments. Appl. Sci. 12, 6340. https://doi.org/10.3390/app12136340

Mohanavelu, A., Naganna, S.R., Al-Ansari, N., 2021. Irrigation Induced Salinity and Sodicity Hazards on Soil and Groundwater: An Overview of Its Causes, Impacts and Mitigation Strategies. Agriculture 11, 983. https://doi.org/10.3390/agriculture11100983

Napo, G., Akpataku, K.V., Seyf-Laye, A.-S.M., Gnazou, M.D.T., Bawa, L.M., Djaneye, G., 2021. Assessment of Shallow Groundwater Quality Using Water Quality Index and Human Risk Assessment in the Vogan-Attitogon Plateau, Southeastern (Togo). J. Environ. Pollut. Hum. Health 9, 50–60.

Ndoye, S., Diedhiou, M., Celle, H., Faye, S., Baalousha, M., Le Coustumer, P., 2023. Hydrogeochemical characterization of groundwater in a coastal area, central western Senegal. Front. Water 4, 1097396. https://doi.org/10.3389/frwa.2022.1097396

Nosrati, K., 2017. Identification of a water quality indicator for urban roof runoff. Sustain. Water Qual. Ecol. 9–10, 78–87. https://doi.org/10.1016/j.swaqe.2017.07.001

Nsabimana, A., Li, P., 2023. Hydrogeochemical characterization and appraisal of groundwater quality for industrial purpose using a novel industrial water quality index (IndWQI) in the Guanzhong Basin, China. Geochemistry 83, 125922. https://doi.org/10.1016/j.chemer.2022.125922

Ogbekene, I., 2025. The Role of Freedom of Expression and Collaborative Governance in Enhancing Community Participation for Water Resource Management in Africa. J. Energy Nat. Resour. 14, 1–11. https://doi.org/10.11648/j.jenr.20251401.11

OMS, 2017. Directives sur la qualité de l’eau de boisson, 4e éd., intégrant le premier additif. ed. Organisation mondiale de la Santé, Genève.

Ouedraogo, I., Girard, A., Vanclooster, M., Jonard, F., 2020. Modelling the Temporal Dynamics of Groundwater Pollution Risks on the African Scale. Water 12, 1406.

Owusu, A., Akpoti, K., Leh, M., Perera, T., Madushanka, L., Mekonnen, K., Tinonetsana, P., Tayebi, N., Escalera-Rodriguez, A.C., Fofana, R., Velpuri, N.M., 2025. Bridging scales and borders on water availability and use in the transboundary Volta River Basin: A water accounting approach. J. Hydrol. Reg. Stud. 59, 102377. https://doi.org/10.1016/j.ejrh.2025.102377

Patel, A., Rai, S.P., Akpataku, K.V., Puthiyottil, N., Singh, A.K., Pant, N., Singh, R., Rai, P., Noble, J., 2023. Hydrogeochemical characterization of groundwater in the shallow aquifer system of Middle Ganga Basin, India. Groundw. Sustain. Dev. 21, 100934. https://doi.org/10.1016/j.gsd.2023.100934

Peiyue, L., Qian, W., Jianhua, W., 2011. Groundwater Suitability for Drinking and Agricultural Usage in Yinchuan Area, China. Int. J. Environ. Sci. 1. https://doi.org/10.6088/ijes.00106020017

Piper, A.M., 1944. A graphic procedure in the geochemical interpretation of water-analyses. Eos Trans. Am. Geophys. Union 25, 914–928. https://doi.org/10.1029/TR025i006p00914

Rai, S.P., Akpataku, K.V., Noble, J., Patel, A., Kumar Joshi, S., 2023. Hydrochemical evolution of groundwater in northwestern part of the Indo-Gangetic Basin, India: A geochemical and isotopic approach. Geosci. Front. 14, 101676. https://doi.org/10.1016/j.gsf.2023.101676

Ramakrishnaiah, C.R., Sadashivaiah, C., Ranganna, G., 2009. Assessment of Water Quality Index for the Groundwater in Tumkur Taluk, Karnataka State, India. J. Chem. 6, 523–530. https://doi.org/10.1155/2009/757424

Rehman, N.U., Ali, W., Muhammad, S., Tepe, Y., 2024. Evaluation of drinking and irrigation water quality, and potential risks indices in the Dera Ismail Khan district, Pakistan. Kuwait J. Sci. 51, 100150. https://doi.org/10.1016/j.kjs.2023.11.001

Renu Nayar, 2020. Assessment of Water Quality Index and Monitoring of Pollutants by Physico-Chemical Analysis in Water Bodies: A Review. Int. J. Eng. Res. V9, IJERTV9IS010046.
https://doi.org/10.17577/IJERTV9IS010046

Rodier, J., Legube, B., Merlet, N., 2009. Analyse de l'eau, 9 ème Edidition. ed. Dunod, Paris.

Saka, D., Adu-Gyamfi, J., Skrzypek, G., Antwi, E.O., Heng, L., Torres- Martínez, J.A., 2023. Disentangling nitrate pollution sources and apportionment in a tropical agricultural ecosystem using a multi-stable isotope model. Environ. Pollut. 328, 121589. https://doi.org/10.1016/j.envpol.2023.121589

Segbeaya, K.N., Koledzi, K.E., Baba, G., Feuilade-Cathalifaud, G., 2019. The impact of household and similar solid wastes on Kara River quality due to their potential to release nitrogen. J. Environ. Chem. Ecotoxicol. 11, 29–42. https://doi.org/10.5897/JECE2019.0447

Şener, Ş., Şener, E., Davraz, A., 2017. Evaluation of water quality using water quality index (WQI) method and GIS in Aksu River (SW-Turkey). Sci. Total Environ. 584–585, 131–144. https://doi.org/10.1016/j.scitotenv.2017.01.102

Shakya, B.M., Nakamura, T., Shrestha, S., Pathak, S., Nishida, K., Malla, R., 2022. Tap Water Quality Degradation in an Intermittent Water Supply Area. Water. Air. Soil Pollut. 233, 81. https://doi.org/10.1007/s11270-021-05483-8

Silva, R.S.B.D., Sousa, A.M.L.D., Sodré, S.D.S.V., Vitorino, M.I., 2018. Avaliação sazonal da qualidade das águas superficiais e subterrâneas na área de influência do Lixão de Salinópolis, PA. Ambiente E Agua - Interdiscip. J. Appl. Sci. 13, 1. https://doi.org/10.4136/ambi-agua.2072

Singh, P., Setia, R., Malik, A., Sekhon, K.S., Mavi, M.S., 2024. Spatio-temporal variations in groundwater quality in the parts of South-western Punjab, India. J. Geochem. Explor. 259, 107417. https://doi.org/10.1016/j.gexplo.2024.107417

Smith, D.N.I., Ortega-Camacho, D., Acosta-González, G., Leal-Bautista, R.M., Fox, W.E., Cejudo, E., 2020. A multi-approach assessment of land use effects on groundwater quality in a karstic aquifer. Heliyon 6, e03970. https://doi.org/10.1016/j.heliyon.2020.e03970

Sodomon, A.K., Akpataku, K.V., Tampo, L., Alfa-Sika Mande, S.-L., Benavente Herrera, J., Martín Rosales, W., Faye, S., 2025. Assessment of hydrogeochemical evolution of groundwater from the basement aquifer in the upper part of transboundary Mono River Basin, Togo. J. Hydrol. Reg. Stud. 58, 102200. https://doi.org/10.1016/j.ejrh.2025.102200

Sunkari, E., Hudu, A., Fosu, S., Gyimah, E., Oppong, O., 2024. Hydrogeochemistry, sources, enrichment mechanism and human health risk assessment of groundwater fluoride in Saboba District in the Oti-sub basin of the Volta River Basin, northern Ghana. Groundw. Sustain. Dev. 101132. https://doi.org/10.1016/j.gsd.2024.101132

Tairou, M.S., Miningou, Y.M.W., Costa, Y.D.D., Kwekam, M., 2022. Petrostructural and Geochemical Characteristics of the Metamagmatites in the External Zone of the Dahomeyides Belt: Case of the Kantè Serpentinites (Northern Togo). Int. J. Geosci. 13, 779–792. https://doi.org/10.4236/ijg.2022.139039

Tampo, L., Alfa-Sika Mande, S.-L., Adekanmbi, A.O., Boguido, G., Akpataku, K.V., Ayah, M., Tchakala, I., Gnazou, M.D.T., Bawa, L.M., Djaneye-Boundjou, G., Alhassan, E.H., 2022. Treated wastewater suitability for reuse in comparison to groundwater and surface water in a peri-urban area: Implications for water quality management. Sci. Total Environ. 815, 152780. https://doi.org/10.1016/j.scitotenv.2021.152780

Tay, C.K., 2021. Hydrogeochemical framework of groundwater within the Asutifi-North District of the Brong-Ahafo Region, Ghana. Appl. Water Sci. 11, 72. https://doi.org/10.1007/s13201-021-01398-1

Tegegne, A.M., Lohani, T.K., Eshete, A.A., 2023. Evaluation of groundwater quality for drinking and irrigation purposes using proxy indices in the Gunabay watershed, Upper Blue Nile Basin, Ethiopia. Heliyon 9, e15263. https://doi.org/10.1016/j.heliyon.2023.e15263

Toi Bissang, B., Akpaki, gouvidé, Baba, G., 2023. Assessment of the Physico-Chemical Quality of Waters in the Canton of Bangeli. Am. J. Water Resour. 11, 126–132. https://doi.org/10.12691/ajwr-11-4-1

Toi Bissang, B., Aragón-Barroso, A.J., Baba, G., González-López, J., Osorio, F., 2024. Integrated Assessment of Heavy Metal Pollution and Human Health Risks in Waters from a Former Iron Mining Site: A Case Study of the Canton of Bangeli, Togo. Water 16, 471. https://doi.org/10.3390/w16030471

Tshanga, M., Mashauri, F., Mashala, P., 2025. Hydrochemical Characteristics of Groundwater in the Mutoshi Deposit Environment, Kolwezi (Lualaba, DR Congo). Adv. Environ. Eng. Res. 06, 1–18. https://doi.org/10.21926/aeer.2502019

UE, 2020. Directive (UE) 2020/2184 Relative à la qualité des eaux destinées à la consommation humaine. J. Off. L'Union Eur.

UNEP-GEF, 2010. Analyse diagnostique transfrontalière du bassin : Rapport National Togo. (Rapport définitif No. 53885). Togo.

UNEP-GEF Volta Project, 2013. Volta Basin Transboundary Diagnostic Analysis (No. 53885).

Wagh, V., Raut, V., Tadse, K., Sahu, U., 2025. Hydrogeochemical evaluation of groundwater in Deccan Volcanic Province, Maharashtra, India through GIS and statistical techniques. Sci. Rep. 15, 32329. https://doi.org/10.1038/s41598-025-17782-9

Xiao, Q., Yu, Q., Huang, F., Chen, F., Zhang, Q., Mi, D., Ye, Q., 2025. Assessing the impacts of motorway construction on groundwater in karst mountain areas, Southwest China. Environ. Technol. Innov. 40, 104338. https://doi.org/10.1016/j.eti.2025.104338

Zoulgami, S., Gnazou, M.D.T., Kodom, T., Djaneye-Boundjou, G., Bawa, L.M., 2015. Physico-chemical study of groundwater in the Northeast of Kara region (Togo). Int J Biol Chem Sci 9, 1711–1724. https://doi.org/10.4314/ijbcs.v9i3.49